An Extension of The Smale-Birkhoff Homoclinic Theorem, Melnikov's Method, and Chaotic Dynamics in Incompressible Fluids

by

Andrea Louise Bertozzi

A thesis
presented to Princeton University
in partial fulfillment of the
requirements for the degree of
Bachelor of Arts
in
Mathematics

Princeton, New Jersey, 1987

Acknowledgements

I would like to thank my advisor, Prof. Andrew Majda, for suggesting the topic and for all the guidance he has given me throughout the year. I would also like to thank John Sullivan for introducing me to TEX and for the generous amount of time he has given in proof reading and in writing the C programs used to generate the graphs in chapters three, four, and five. In addition, I would like to thank Tom Parks for his assistance in creating the diagrams.

I would especially like to thank my parents for all their kindness and support.

Abstract

The Smale-Birkhoff Homoclinic Theorem and Melnikov's Method are two very useful tools for studying the onset of chaos and the complicated mixing patterns that sometimes occur in time-periodic perturbations of certain planar dynamical systems. The homoclinic theorem proves the existence of a subsystem topologically equivalent to the shift on two symbols occurring in certain maps possessing a homoclinic orbit to a hyperbolic saddle point. Melnikov's method provides a direct way of calculating when such maps will occur in a perturbed planar dynamical system. This method, coupled with the homoclinic theorem, has been widely used to study the onset of chaos in many dynamical systems containing homoclinic orbits (See Guckenheimer and Holmes [1983] pp.184-193,426 for a discussion of the many applications that have been studied). We extend the planar homoclinic theorem to the case of a heteroclinic orbit connecting a finite number of saddle points. This extension will enable us to apply Melnikov's method to some interesting systems with heteroclinic cycles as well as ones with homoclinic orbits.

Many interesting two dimensional fluid dynamical models can be viewed as planar dynamical systems with heteroclinic saddle connections. We study the Kelvin-Stuart Cat's Eye flow, a well known model for a pattern found in shear layers. This model is a planar dynamical system possessing an infinite number of heteroclinic saddle connections involving two fixed points each. We also study a planar lattice flow in which we find groups of four saddle points linked by heteroclinic orbits. The lattice flow is an interesting model for certain convection patterns as well as for nonlinear Taylor vortex flow. In the unperturbed case, the above two flows are steady solutions to the inviscid Euler equations and thus have a direct Hamiltonian formulation. We thus apply the simplified Hamiltonian formulation of Melnikov's method to find chaotic motion and mixing occurring in time periodic perturbations of these two planar flows.

The third application of Melnikov's method presented here is of a somewhat different nature from the first two. We examine the evolution equations for an elliptical vortex in a imposed strain. These equations have a Hamiltonian form based on a dimensionless time parameter. The most physically interesting perturbations are

based on real time and so we are forced to study a non-Hamiltonian dynamical system with a homoclinic orbit. We apply the non-Hamiltonian version of Melnikov's method to find chaotic dynamics occurring in the case of periodic stretching of the straining flow in a third dimension.

Contents

0 Background Information

0.1 Dynamical Systems

A good introduction to dynamical systems can be found in the paper by Guckenheimer [1979]. Guckenheimer and Holmes [1983] present a thorough account for the reader who is more familiar with the standard terminology.

Dynamical systems come in two forms, the discrete case and the continuous case. A discrete dynamical system on a manifold M is a diffeomorphism $\varphi : M \longrightarrow M$. We obtain a discrete family (φ, M) by taking φ and its iterates φ^k where $k \in \mathbb{Z}$. In the continuous case, we have a one parameter group of diffeomorphisms φ_t that vary continuously in time. A continuous family will yield a discrete family by fixing some time t_0 and setting $\varphi = \varphi_{t_0}$. Locally, we characterize φ_t by a differential equation $\dot{x} = f(x)$ where $x \in M$. φ_t is then the solution to the equation

$$\frac{d}{dt}(\varphi_t(x))|_{t=\tau} = f(\varphi_\tau(x)).$$

Such a system is called autonomous is that the vector field of the flow is time independent.

Given a nonautonomous system of the form

$$\dot{x} = f(x,t) \quad x \in M,$$

we can turn this into an autonomous system on $M \times \mathbb{R}$:

$$\begin{aligned} \dot{x} &= f(x,s) \\ \dot{s} &= 1 \qquad (x,s) \in M \times \mathbb{R}. \end{aligned}$$

In the case where $f(x,t) = f(x,t+T)$ i.e. f is T-periodic in time, we have the autonomous system:

$$\begin{aligned} \dot{x} &= f(x,\theta) \\ \dot{\theta} &= 1 \qquad (x,s) \in M \times S^1. \end{aligned}$$

0.2 Fixed Points, Stable and Unstable Manifolds

Given a dynamical system $\dot{x} = f(x)$, a point x_0 where $f(x_0) = 0$ is called a *fixed point.* In the neighborhood of a fixed point, the flow is approximated by the linear system $\dot{\xi} = Df(x_0)\xi$. Here, Df denotes the Jacobian matrix $[\partial f_i/\partial x_j]$. If $Df(x_0)$ has no eigenvalues with zero real part, x_0 is called a *hyperbolic* fixed point and the asymptotic behavior of the system near x_0 is governed by the linearized equation. In particular, the local stable and unstable manifolds are approximated by the eigenspaces of Df. We define the *stable and unstable manifolds* as follows:

$$W^s(x_0) = \{x \in M \quad | \quad \varphi_t(x) \to x_0 \quad as \quad t \to \infty\},$$
$$W^u(x_0) = \{x \in M \quad | \quad \varphi_t(x) \to x_0 \quad as \quad t \to -\infty\}.$$

In the discrete case a fixed point of φ is simply one that satisfies $\varphi(x_0) = x_0$. The fixed point is hyperbolic if $D\varphi|_{x_0}$ has no eigenvalues of unit modulus. In such a case we define the stable and unstable manifolds of x_0 by

$$W^s(x_0) = \{x \in M \quad | \quad \varphi^k(x) \to x_0 \quad as \quad k \to \infty\},$$
$$W^u(x_0) = \{x \in M \quad | \quad \varphi^k(x) \to x_0 \quad as \quad k \to -\infty\}.$$

0.3 Poincaré Maps

Suppose we have a periodic orbit γ of a flow φ_t in $\mathbb{R}^n$. Let Σ be a local cross section of dimension $n-1$ so that the flow is everywhere transverse to Σ. Formally, this means that $f(x) \cdot \vec{n}(x) \neq 0, \quad \forall x \in \Sigma$, where $n(x)$ is the unit normal to Σ at x.

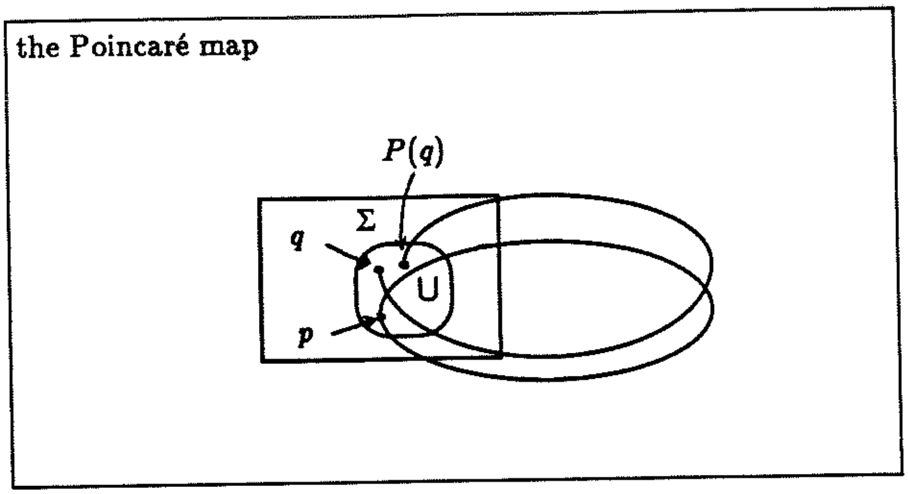

Given $U \subset \Sigma$, a neighborhood of $p \in \gamma$, define the Poincaré map $P : U \longrightarrow \Sigma$ by $P(q) = \varphi_\tau(q)$ where $\tau = \tau(q)$ is the smallest time t for which $\varphi_t(q)$ returns to Σ. Here τ depends smoothly on q and is in general not T, the period of γ. However, $\tau \to T$ as $q \to p$.

0.4 Planar Fluid Flow and Hamiltonian Systems

A planar autonomous Hamiltonian system is of the form

$$\dot{x} = -\frac{\partial H}{\partial y}$$
$$\dot{y} = \frac{\partial H}{\partial x}$$

where H is a function of x and y. Streamlines of the flow are simply constants of H. The Euler equation describing the motion of an ideal, non-viscous fluid is

$$\rho \frac{D\vec{u}}{Dt} = -\nabla p + \vec{F}.$$

Here, $\vec{u}$ is the vector fluid velocity, p the pressure, ρ the fluid density and $\vec{F}$, an external force. $DA/Dt = \partial A/\partial t + (u \cdot \nabla)A$ is the convective derivative. Let $\omega = \nabla \times u$ be the vorticity. For a two dimensional incompressible flow with conservative force, we have $\nabla \cdot \vec{u} = 0, \quad \nabla \times \vec{F} = 0$. We take the curl of the Euler equation to obtain the vorticity equation

$$\frac{D\omega}{Dt} = 0.$$

In two dimensions, define $\vec{u} = (u, v)$. We have a scalar vorticity $\omega = \partial_x v - \partial_y u$. By incompressibility, $\nabla \cdot u = 0$ which implies that $\partial_x u = -\partial_y v$. Thus, there exists a stream function $\Psi(x, y, t)$ so that

$$u = \partial_y \Psi, \quad v = -\partial_x \Psi.$$

For a steady flow, Ψ is time independent and the velocity of the fluid describes a planar Hamiltonian flow. We see that for a general ideal planar flow,

$$\omega = -\Delta \Psi.$$

In the case of an irrotational flow, $\omega = 0$ and $u + iv$ satisfies the Cauchy-Riemann equations. The fluid velocity defines an analytic function in the complex plane.

Discussion of the Euler equations and vorticity in ideal fluids can be found in Chorin and Marsden pp. 24-42. A mathematical discussion of the general stream function in hydrodynamics can be found in Arnold [1984] pp. 333-337.

1 Extension of the Homoclinic Theorem

The ideas for the homoclinic theorem were first laid out by Birkhoff [1935]and were developed by Smale [1963]. We consider a planar diffeomorphism φ possessing a hyperbolic saddle point p whose stable and unstable manifolds intersect transversely at a point q (see fig. 1.1). A result of this theorem is that φ possesses a subsystem equivalent to a shift on two symbols.

figure 1.1

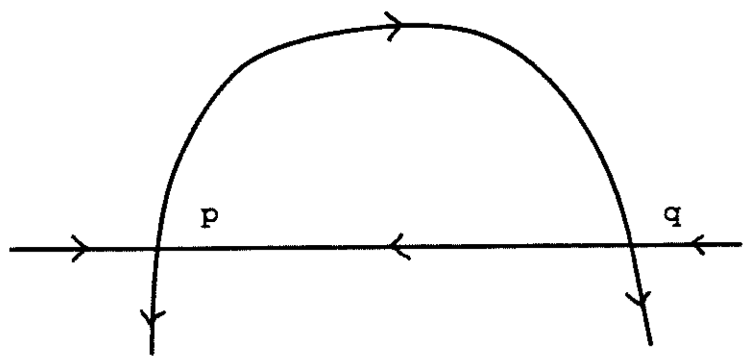

We extend this theorem to the case of N fixed points joined by transverse saddle connections (see fig. 1.5). The homoclinic theorem is proved by constructing the horseshoe map and showing that it possesses the shift as a subsystem. One must then show that φ posses the horseshoe map as a subsystem. We construct the generalized horseshoe map, expanding on the machinery of Moser [1973] in his description of the map on the unit square. Using a combination of ideas from the proofs of the homoclinic theorem as outlined in Moser and Guckenheimer and Holmes [1983], We prove the heteroclinic theorem by exhibiting a subsystem in φ equivalent to the generalized horseshoe map.

1.1 The Horseshoe map and the Shift on Two Symbols

We first define the horseshoe map used in the homoclinic case.

figure 1.2

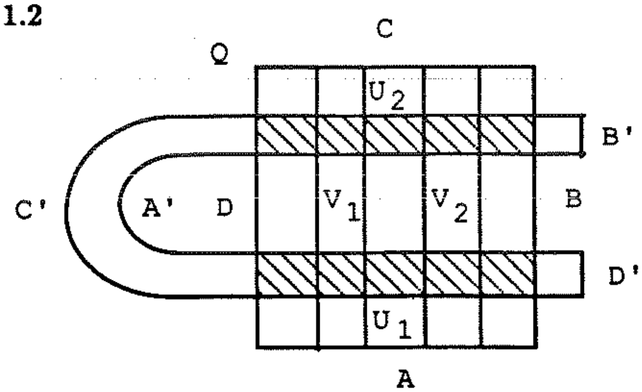

The Horseshoe Map

The horseshoe map is a topological mapping of the unit square Q into the plane such that $\varphi(Q) \cap Q$ has two components U_1, U_2. The preimages of U_1 and U_2 are denoted by $V_i = \varphi^{-1}(U_i), \quad i = 1, 2$. V_1 and V_2 correspond to vertical strips connecting the upper and lower edges of Q (see fig. 1.2). The iterates φ^k of φ are not defined in all of Q, so we construct the invariant set

$$I = \bigcap_{k=-\infty}^{\infty} \varphi^{-k}(Q),$$

in which all iterates φ^k are defined. Associated with each point p of I is a bi-infinite sequence $(...s_{-1}, s_0; s_1, s_2...)$, $\quad s_i \in \{1,2\}$ of ones and twos. Where $\varphi^{-k}(p) \in V_{s_k}$ or

$$p \in \bigcap_{k=-\infty}^{\infty} \varphi^k(V_{s_k}).$$

On the set S of all such sequences, we define a map σ by $(\sigma s)_i = s_{i+1}$. All the elements of s are shifted over by one. This provides a mapping $\tau : I \rightarrow S$ with $\tau\varphi \mid_I = \sigma\tau$ as long as τ is invertible. We introduce a topology on S as follows: Given $s^* = (..., s^*_{-2}, s^*_{-1}, s^*_0; s^*_1, s^*_2, ...) \in S$ then $U_j = \{s \in S | s_k = s^*_k, \quad (|k| < j)\}$ form a neighborhood basis for s^*. We see that the horseshoe map possesses periodic orbits of arbitrary period, as well as an orbit which comes arbitrarily close to all points of I. This last orbit is obtained by constructing a sequence which contains all possible finite strings of 1's and 2's.

1.2 A Generalization of the Horseshoe Map

Consider a set of N disjoint squares Q_N in the plane and a map $\varphi : \bigcup Q_N \to \mathbb{R}^2$ such that $\varphi(Q_i) \cap Q_i$ is a horizontal strip in Q_i and $\varphi(Q_i) \cap Q_{i+1} \pmod N$ is a horizontal strip in $Q_{i+1} \pmod N$.

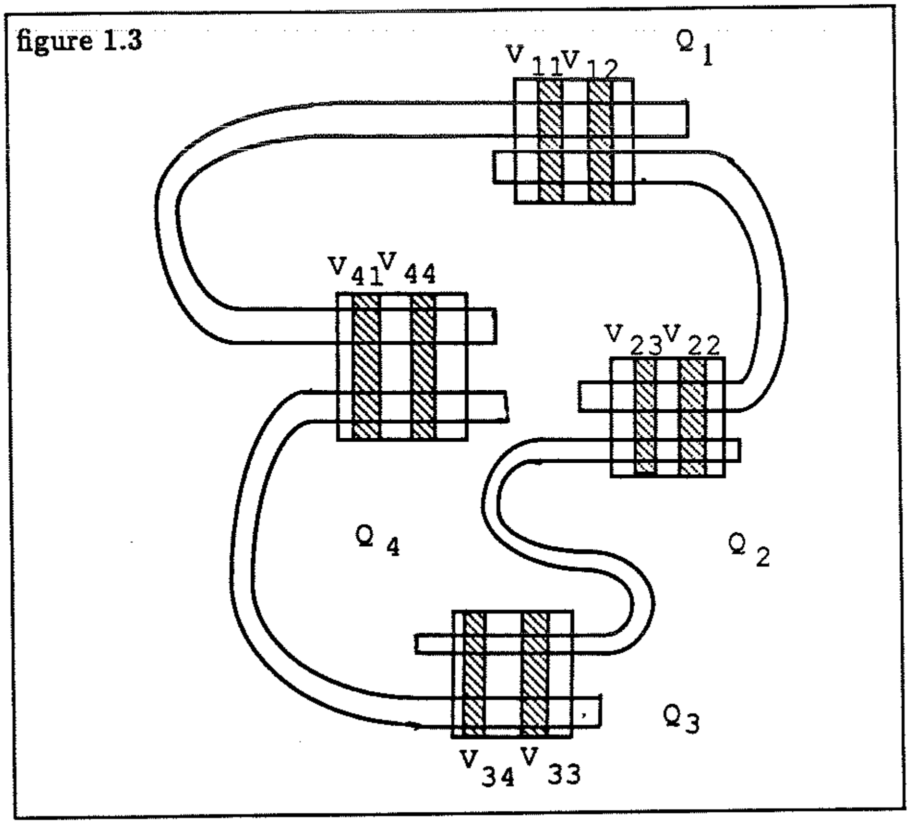

figure 1.3

Here it is not important how each square Q_i is oriented with respect to the other squares, only that $\varphi(\bigcup_i Q_i) \cap Q_j$ are horizontal strips in Q_j. Our invariant set will thus be

$$I = \bigcap_{k=-\infty}^{\infty} \varphi^{-k}(\bigcup_i Q_i).$$

We will associate with each point $p \in I$ a bi-infinite sequence $(..., s_{-1}, s_0; s_1, s_2...) \in S'$ of N consecutive symbols where

$$S' = \{s | s_i \in (1, .., N), \quad s_{i+1} = s_i \quad or \quad s_{i+1} = s_i + 1 \pmod N)$$

such that $\varphi^{-k}(p) \in Q_{s_k}$. Under the appropriate conditions we want to show that there is a one to one correspondence between points of I and sequences $s \in S'$.

We must introduce some definitions to make the above ideas more precise. Given a square Q in the plane, introduce local coordinates x and y on Q so that Q becomes the unit square (see fig. 1.4).

figure 1.4

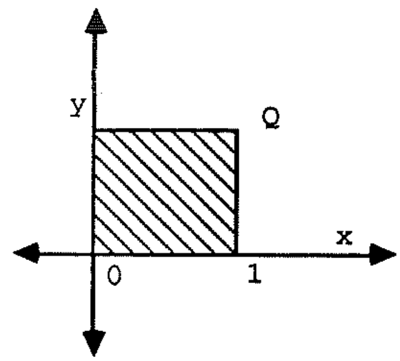

Given $0 < \mu < 1$, we say that $y = u(x)$ is a horizontal curve if $0 \leq u(x) \leq 1$ for $0 \leq x \leq 1$ and $|u(x_1) - u(x_2)| \leq \mu|x_1 - x_2|$ for $0 \leq x_1 \leq x_2 \leq 1$. If u_1 and $u_2(x)$ define two such horizontal curves and if $0 \leq u_1(x) < u_2(x) \leq 1$ then

$$U = \{(x, y)|0 \leq x \leq 1; u_1(x) \leq y \leq u_2(x)\}$$

is called a horizontal strip. Define $d(U) = \max_{0\leq x\leq 1}(u_2(x) - u_1(x))$ to be the diameter of U. Similarly, a vertical curve $x = v(y), \quad 0 \leq y \leq 1, \quad 0 \leq v(y) \leq 1$ has $|v(y_1) - v(y_2)| \leq \mu|y_1 - y_2|$ in $0 \leq y_1 \leq y_2 \leq 1$. A vertical strip is defined in the same way as is a horizontal strip.

Lemma 1.2.1. *Given horizontal strips $U_1, U_2, \ldots$ in Q with $U_i \subset U_{i-1}$, if $d(U_i) \to 0$ as $i \to \infty$ then $\bigcap_{n=1}^{\infty} U_n$ is a horizontal curve.*

Proof: This follows because horizontal curves are compact. A similar result holds for vertical strips.

Lemma 1.2.2. *A horizontal curve $y = u(x)$ and a vertical curve $x = v(y)$ intersect in exactly one point.*

Proof: A point of intersection (x, y) is a zero x of $x - v(u(x))$. Also,

$$\begin{aligned} |v(u(x_1)) - v(u(x_2))| &\leq \mu |u(x_1) - u(x_2)| \\ &\leq \mu^2 |x_1 - x_2| \\ \mu^2 &< 1. \end{aligned}$$

Thus $x - v(u(x))$ is strictly monotonically increasing. Furthermore, $x - v(u(x)) \leq 0$ for $x = 0$ and is ≥ 0 for $x = 1$. Thus $x - v(u(x))$ has precisely one zero.

We can now precisely define our map φ: Let $Q_1, Q_2, ..., Q_N$ be disjoint rectangles in the plane. Let x_i, y_i be local coordinates for Q_i such that Q_i is the unit square in x_i, y_i and φ is a linear map in Q_i. We further assume:

(A1) Let $V_{11}, V_{12}, V_{22}, V_{23}, ..., V_{NN}, V_{N1}$ be $2N$ disjoint vertical strips with $V_{ij} \subset Q_i$. Let $U_{11}, U_{12}, U_{22}, U_{23} ..., U_{NN}, U_{N1}$ be $2N$ disjoint horizontal strips with $U_{ij} \in Q_j$. We require that $\varphi(V_{ij}) = U_{ij}$: Moreover, we require that vertical boundaries of V_{ij} get mapped to vertical boundaries of U_{ij}, and the same holds true for horizontal boundaries (see fig. 1.3).

(A2) If V is a vertical strip in Q_j then for $i \equiv j$ or $i \equiv j-1 \pmod N$, $\varphi^{-1}(V) \cap V_{ij} = \widetilde{V}_{ij}$ is a vertical strip in Q_i and for some fixed ν $(0 < \nu < 1)$, we have $d(\widetilde{V}_{ij}) \leq \nu d(V_{ij})$. Similarly, if U is a horizontal strip in Q_i, then for $j \equiv i$ or $j \equiv i + 1 \pmod N$ we require that $\varphi(U) \cap U_{ij} = \widetilde{U}_{ij}$ is a horizontal strip in Q_j with $d(\widetilde{U}_{ij}) \leq \nu d(U_{ij})$.

We have the following theorem:

Theorem 1.2.1. *If φ is a homeomorphism in the plane satisfying the above assumptions (A1) and (A2), then it contains the shift σ on the sequences in S as a subsystem. There exists a homeomorphism $\tau : (\bigcup Q_i) \longrightarrow S$ such that $\sigma\tau = \tau\varphi$. In particular, $\tau^{-1}(S)$ is a closed invariant set in $\bigcup Q_i$.*

Proof: We will construct the map $\tau^{-1} : S \longrightarrow \bigcup Q_i$ and then show that it satisfies the necessary properties.

Given $s = (..., s_{-1}, s_0; s_1, s_2...) \in S$ define $V_{s_0} = Q_{s_0}$ now define inductively $V_{s_0 s_1 ... s_m} = V_{s_0} \cap \varphi - 1(V_{s_1 s_2 ... s_m})$ for $m \geq 2$. By the assumptions, $d(V_{s_0 s_1 ... s_m}) \leq \nu^m$ so $d(V_{s_0 s_1 ... s_m}) \to 0$ as $m \to \infty$. Also

$$V_{s_0 s_1 ... s_m} = \{p \in \bigcup Q_i, \varphi^k(p) \in Q_{s_k}(k = 1, ..., m)\}$$

defines a vertical strip in Q_{s_0}. By Lemma 1.2.1, $V(s) = \lim_{m \to \infty}(V_{s_0 s_1 ... s_m})$ is a vertical curve in Q_{s_0}.

Defining $U(s)$ analogously, we can apply Lemma 1.2.2 to determine that the two curves intersect in exactly one point, $\tau^{-1}(s)$. Thus, we see that tau^{-1} is well defined, thus τ is on-to-one. It remains to show that τ and τ^{-1} are continuous. If s and s' agree in the kth components for $|k| < m$, then $\tau^{-1}(s)$, $\tau^{-1}(s')$ both belong to $V_{s_0 s_1 s_2 ... s_m}$ and $U_{s_0 s_{-1} ... s_{-m}}$. Since $d(V_{s_0 s_1 ... s_m}) \leq \nu^m$ and $d(U_{s_0 s_{-1} ... s_{-m}}) \leq \nu^m$, we have $|\tau^{-1}(s) - \tau^{-1}(s')| \leq 2(1 - \mu_{s_0})^{-1}\nu^m$. Thus τ is continuous. Since τ^{-1} is one to one continuous on a compact set, τ is continuous.

As part of the analysis in the following section, we use the following case of a lemma due to Palis [1969]. We state it here without proof:

λ-lemma. *Given a planar diffeomorphism φ possessing a hyperbolic fixed point p and a point q where the stable and unstable manifolds of p intersect transversely, then for any ball B^r around p in $W^u(p)$ and any $\varepsilon > 0$, then there exists a ball $B^{\bar{r}}$ in $W^u(p)$, intersecting $W^s(p)$ transversely, which under iterates of φ becomes ε close to B^r.*

1.3 A Heteroclinic Theorem

Theorem 1.3.1. *If a diffeomorphism $\varphi : \mathbb{R}^2 \longrightarrow \mathbb{R}^2$ possesses N fixed points $p_1, p_2, ..., p_N$ that are non-degenerate hyperbolic saddle points, and there exist points q_i at which the unstable manifold $W^u(p_i)$ intersects the stable manifold $W^s(p_{i+1 \pmod N})$ transversely for all i, then φ possesses an invariant set I on which some iteration φ^k is homeomorphic to the shift on S', the set of bi-infinite sequences of N consecutive symbols (as described in the preceding section).*

proof: We want to show that φ possesses a subsystem satisfying the requirements for the generalized horseshoe map of section 1.2. The stable and unstable manifolds are depicted in fig. 1.5.

figure 1.5

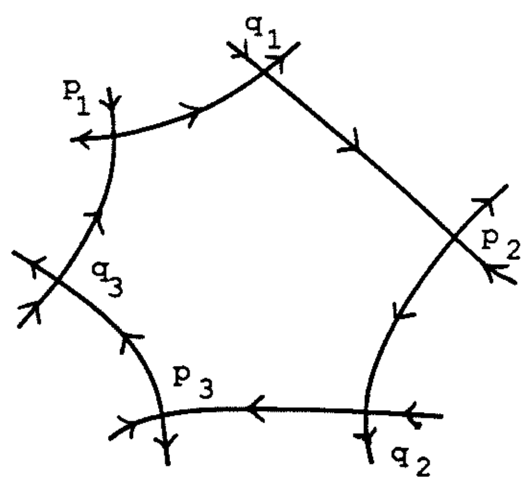

Claim: we can choose an integer k and neighborhoods U_i of p_i such that the following conditions are satisfied (see fig. 1.6):

(1) There exists a local coordinate system in U_i so that φ is linear, and U_i is the unit square.
(2) $q_i \in \varphi^k(U_i)$ and $q_i \in \varphi^{-k}(U_{i+1 \pmod N})$ for all i.
(3) For $R_i = \varphi^k(U_i) \cap \varphi^{-k}(U_{i+1 \pmod N})$, we have $\varphi^{-k}(R_i \cap W^s(p_{i+1 \pmod N}))$ intersects $\varphi^k(R_{i-1 \pmod N} \cap W^u(p_{i-1 \pmod N})$ transversely in exactly one point.

figure 1.6

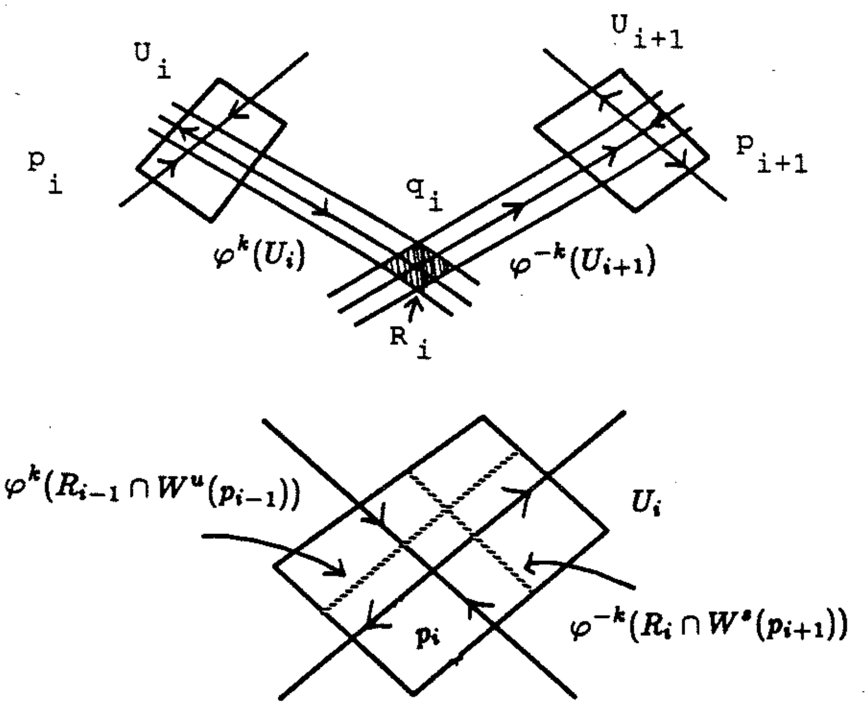

We choose U_i so that (1) is satisfied for all i. Note that if we shrink each U_i, (1) will still hold. Given any U_i satisfying (1), by the definition of stable and unstable manifolds, there exists a k such that (2) is satisfied. Note that k depends on the sizes of the U_i, which we will continue to shrink until all the above conditions are satisfied. By the λ-lemma of Palis, $\varphi^{-k}(R_i \cap W^s(p_{i+1 \pmod N}))$ approaches $W^s(p_i)$ and $\varphi^k(R_{i-1 \pmod N} \cap W^u(p_{i-1 \pmod N})$ approaches $W^u(p_i)$ as $k \to \infty$. Thus for k sufficiently large and the U_i sufficiently small, (3) is satisfied. Transversal intersection results because $W^s(p_i)$ and $W^u(p_i)$ intersect transversely at p_i. Once (3) is achieved, we can find U_i sufficiently small so that there exists μ_i for each p_i

so that $\varphi^{-k}(R_i)$ is a vertical strip and $\varphi^k(R_{i-1 \pmod N})$ is a horizontal strip in U_i. By our construction, we are assured that horizontal boundaries get mapped to horizontal boundaries and vertical boundaries get mapped to vertical boundaries. We have showed that φ^{2k} satisfies the first assumption (A1) of theorem 1.2.1. The second assumption is easily fulfilled by the local compression properties of φ^{-1}. There are a finite number of vertical strips. Since φ is linear in each U_i, the part of a strip that stays in U_i automatically get compressed by some fixed amount. The part of a vertical strip that travels from U_i to U_j along $W^s(p_i)$ and $W^u(p_j)$ will be compressed as it travels along each piece, as we see in the diagram. Thus, there exists some $0 < \nu < 1$ such that $d(\widetilde{V}_{ij}) \leq \nu d(V_{ij})$ for $\varphi^{-1}(V) \cap V_{ij} = \widetilde{V}_{ij}$. A similar result holds for the horizontal strips. We have satisfied both assumptions (A1) and (A2) of theorem 1.2.1. Thus, φ^{2k} possesses a subsystem equivalent to the generalized horseshoe map which in turn possesses a subsystem topologically equivalent to the shift on N consecutive symbols.

This last subsystem is termed "chaotic" because of the interesting properties it exhibits under iterations of φ^{2k}. We have orbits of arbitrary period greater than N as well as dense orbits. The bi-infinite sequence corresponding to a dense orbit is formed by concatenating all possible finite sequences of consecutive symbols. We further note the unpredictability of this subsystem. Any two orbits whose sequences are the same for some finite length, may have completely different sequences further on. Physically we will find these orbits near each other under a finite number of iterations of φ^{2k}, yet the orbits diverge as we proceed past the point where their sequences agree. Thus, knowing where a point will be for a fixed finite time in no way predicts where it will be at later times.

2 Melnikov's Method

Now that we know that the planar diffeomorphisms of theorem 1.3.1 yield wild chaotic patterns, we would like to find a way of determining whether or not a specific map satisfies the conditions of this theorem. Melnikov [1963] devised a method for finding transversal intersection of stable and unstable manifolds given a time-periodic perturbation of a system with a saddle connection. Here we present Melnikov's method in a style similar to that of Guckenheimer and Holmes [1983] (pp. 184-9). We generalize their presentation to the case of a heteroclinic saddle connection in a system that is not necessarily Hamiltonian.

2.1 The Poincaré map and the Melnikov function

Consider the planar dynamical system:

$$\text{(A)} \quad \dot{x} = f(x) + \varepsilon g(x,t) \quad x \in \mathbb{R}^2, \quad g(x,t) = g(x,t+T), \quad 0 \le \varepsilon << 1$$

where for $\varepsilon = 0$ we have a saddle connection Γ_0 between two nondegenerate hyperbolic saddle points p_1 and p_2:

figure 2.1

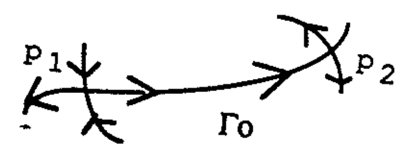

The unstable manifold $W_0^u(p_1)$ of p_1 and the stable manifold $W_0^s(p_2)$ of p_2 coincide. Here we include the homoclinic case where $p_1 = p_2$. Associated with (A) is the suspended system

$$\text{(B)} \quad \dot{x} = f(x) + \varepsilon g(x,\theta), \quad (x,\theta) \in \mathbb{R}^2 \times S^1, \quad (S^1 = \mathbb{R}/T).$$

For ε sufficiently small, (B) possesses a Poincaré map: $P_\varepsilon^{t_0} : \Sigma_{t_0} \longrightarrow \Sigma_{t_0}$ where $\Sigma_{t_0} = \{(x,\theta) \in \mathbb{R}^2 \times S^1 | \theta = t_0\}$ is a global cross section of the flow. Let $F_t^\varepsilon(x_0, t_0)$ be the flow map of (B) on $\mathbb{R} \times S^1$. $P_\varepsilon^{t_o}$ is obtained by a projection onto the first factor: $P_\varepsilon^{t_0}(x) = \pi(F_T^\varepsilon(x, t_0))$ where $\pi((x,\theta)) = x$. Here $P_\varepsilon^{t_0}$ is a map from $\mathbb{R}^2$ to $\mathbb{R}^2$.

Our assumptions imply that for $\varepsilon = 0$, $P_\varepsilon^{t_0}(x)$ has fixed points at p_1 and p_2 and so the suspended system has circular orbits $\gamma^1 = p_1 \times S^1, \gamma^2 = p_2 \times S^1$ with stable and unstable manifolds $W_0^u(\gamma^1)$ and $W_0^s(\gamma^2)$ intersecting to form a "cylinder" $\Gamma_0 \times S^1$. Such saddle connections are quite unstable and are thus expected to break under small perturbations.

However, for ε sufficiently small, we have perturbed saddle points $p_\varepsilon^1, p_\varepsilon^2 \in \Sigma_{t_0}$ which possess local stable and unstable manifolds $W_\varepsilon^u(p_\varepsilon^1), W_\varepsilon^s(p_\varepsilon^2)$ close to $W_0^u(p_1), W_0^s(p_2)$. Using the implicit function theorem, invariant manifold theory, and standard Gronwall estimates, we have the following two results:

For ε sufficiently small,

(1.3.1) The Poincaré map $P_\varepsilon^{t_0}$ has unique hyperbolic saddle points $p_\varepsilon^1 = p_1 + \mathcal{O}(\varepsilon), p_\varepsilon^2 = p_2 + \mathcal{O}(\varepsilon)$.

(1.3.2) Orbits $q_\varepsilon^s(t,t_0)$ and $q_\varepsilon^u(t,t_0)$ lying in $W^s(\gamma_\varepsilon^2)$ and $W^u(\gamma_\varepsilon^1)$ and based on Σ_{t_0} can be expressed as follows:

$$q_\varepsilon^u(t,t_0) = q^0(t-t_0) + \varepsilon q_1^u(t,t_0) + \mathcal{O}(\varepsilon^2); \quad t \in [t_0, \infty),$$
$$q_\varepsilon^s(t,t_o) = q^0(t-t_0) + \varepsilon q_1^s(t,t_0) + \mathcal{O}(\varepsilon^2); \quad t \in (-\infty, t_0],$$

where q_0 is the solution to the unperturbed system that coincides with Γ_0.

The above statements imply that q_1^s and q_1^u are uniformly approximated by solutions to the equations:

$$\dot{q}_1^s(t,t_0) = Df(q^0(t-t_0))q_1^s(t,t_0) + g(q^0(t-t_0),t); \quad t \geq t_0$$

$$\dot{q}_1^u(t,t_0) = Df(q^0(t-t_0))q_1^u(t,t_0) + g(q^0(t-t_0),t); \quad t \leq t_0.$$

We define

$$q_\varepsilon^u(t_0) = q_\varepsilon^u(t_0, t_0),$$
$$q_\varepsilon^s(t_0) = q_\varepsilon^s(t_0, t_0),$$
$$d(t_0) = q_\varepsilon^u(t_0) - q_\varepsilon^s(t_0).$$

We have that $q_\varepsilon^u(t_0)$, $q_\varepsilon^s(t_0)$ are approximated by the unique points on $W^u(p_\varepsilon^1)$ and $W^s(p_\varepsilon^2)$ lying on the normal $f^\perp(q^0(0)) = (-f_2(q^0(0)), f_1(q^0(0)))^T$ to Γ^0 at $q^0(0)$, closest to $q^0(0)$ (see fig. 2.2). (1.3.2) Implies that

$$d(t_0) = \varepsilon \frac{f(q^0(0)) \wedge (q_1^u(t_0) - q_1^s(t_0))}{|f(q^0(0))|} + O(\varepsilon^2),$$

where $a \wedge b = a_1 b_2 - b_1 a_2$.

figure 2.2

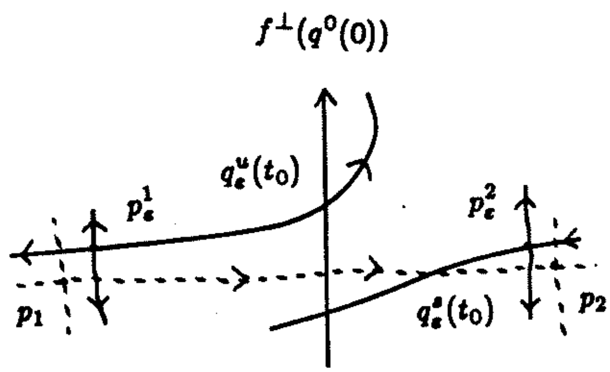

Define the Melnikov function:

$$M(t_0) = \int_{-\infty}^{\infty} f(q^0(t-t_0)) \wedge g(q^0(t-t_0), t) \exp\Big(\int_0^{t-t_0} trDf(q^0(s))ds\Big) dt.$$

In the case where the unperturbed system is Hamiltonian, we have $trDf(q^0) = 0$ and the Melnikov function becomes

$$M(t_0) = \int_{-\infty}^{\infty} f(q^0(t-t_0)) \wedge g(q^0(t-t_0), t)dt$$

The examples of sections 3 and 4 are both Hamiltonian systems. Two useful forms for computation are:

$$M(t_0) = \int_{-\infty}^{\infty} f(q^0(t)) \wedge g(q^0(t), t+t_0) \exp\Big(\int_0^t trDf(q^0(s))ds\Big)dt$$

in the non-Hamiltonian case and

$$M(t_0) = \int_{-\infty}^{\infty} f(q^0(t)) \wedge g(q^0(t), t+t_0)dt$$

in the Hamiltonian case. We note that $M(t_0)$ is itself a periodic function in t_0. Using the second form, we have that

$$\begin{aligned} M(t_0+T) &= \int_{-\infty}^{\infty} f(q^0(t)) \wedge g(q^0(t), t+t_0+T) \exp\Big(\int_0^t trDf(q^0(s))ds\Big)dt \\ &= \int_{-\infty}^{\infty} f(q^0(t)) \wedge g(q^0(t), t+t_0) \exp\Big(\int_0^t trDf(q^0(s))ds\Big)dt \\ &= M(t_0), \end{aligned}$$

since $g(x, t+T) = g(x, t)$.

2.2 Melnikov's Theorem

Melnikov's Theorem. *Given the above conditions, and ε sufficiently small, if $M(t_0)$ has simple zeros, the $W^s_\varepsilon(p^2_\varepsilon)$ and $W^u_\varepsilon(p^1_\varepsilon)$ intersect transversely. If $M(t_0)$ has no zeros in $t_0 \in [0,T]$ then $W^s_\varepsilon(p^2_\varepsilon) \cap W^u_\varepsilon(p^1_\varepsilon) = \emptyset$.*

proof of Melnikov's Theorem:

Define $\Delta(t,t_0) = f(q^0(t-t_0)) \wedge (q^u_1(t,t_0) - q^s_1(t,t_0)) = \Delta^u(t,t_0) - \Delta^s(t,t_0)$. Thus

$$\varepsilon\frac{\Delta(t_0,t_0)}{|f(q^0(0))|} + \mathcal{O}(\varepsilon^2) = d(t_0).$$

Also, $\dot{\Delta}^s(t,t_0) = Df(q^0(t-t_0))\dot{q}^0(t-t_0) \wedge q^s_1(t,t_0) + f(q^0(t-t_0) \wedge \dot{q}^s_1(t,t_0)$. Since $\dot{q}^0 = f(q^0)$, we have $\dot{\Delta}^s = Df(q^0)f(q^0) \wedge q^s_1 + f(q^0) \wedge (Df(q^0)q^s_1 + g(q^0,t)) = trDf(q^0)(\Delta^s) + f(q^0)^g(q^0,t)$. Solving this ODE for Δ^s, we obtain:

$$\Delta^s(\infty,t_0) - \Delta^s(t_0,t_0)$$

$$= \int_{t_0}^{\infty} f(q^0(t-t_0)) \wedge g(q^0(t-t_0),t)\exp\Big(\int_0^{t-t_0} trDf(q^0(s))ds\Big)dt.$$

However, $\Delta^s(\infty,t_0) = \lim_{t\to\infty} f(q^0(t-t_0)) \wedge q^s_1(t,t_0) = 0$ since $f(p_2) = 0$ and $q^0(t-t_0) \to p_2$ as $t \to \infty$. Similarly, we have that $\Delta^u(t_0,t_0)$

$$= \int_{-\infty}^{t_0} f(q^0(t-t_0)) \wedge g(q^0(t-t_0),t)\exp\Big(\int_0^{t-t_0} trDf(q^0(s))ds\Big)dt.$$

Thus we have $\Delta(t_0,t_0) = M(t_0)$. Since $d(t_0) = \mathcal{O}(\varepsilon)M(t_0) + \mathcal{O}(\varepsilon^2)$, if $M(t_0)$ changes sign, then $(q^u_1(t_0) - q^s_1(t_0))$ must change sign, indicating a value t where $q^u_\varepsilon(t,t_0) = q^s_\varepsilon(t,t_0)$. $W^u_\varepsilon(p^1_\varepsilon)$ and $W^s_\varepsilon(p^2_\varepsilon)$ must intersect, and will do so transversely if $M(t_0)$ has simple zeros.

3 Kelvin-Stuart Cat's Eye Flow

Consider the following flow in the plane:

$$\dot{x} = \frac{a \sinh y}{a \cosh y + \sqrt{a^2 - 1} \cos x}$$

$$\dot{y} = \frac{\sqrt{a^2 - 1} \sin x}{a \cosh y + \sqrt{a^2 - 1} \cos x}$$

This is a Hamiltonian system with $H_0 = \log(a \cosh y + \sqrt{a^2 - 1} \cos x)$. It is a model for a pattern found in shear layer flow (see Stuart [1971] and Holm, Marsden, and Ratui [1979]). The parameter a controls the shape of the cat's eye with a larger a corresponding to wider "eyes". Here we consider only $a > 1$. Streamlines are constants of H_0 (see fig. 3.1).

figure 3.1

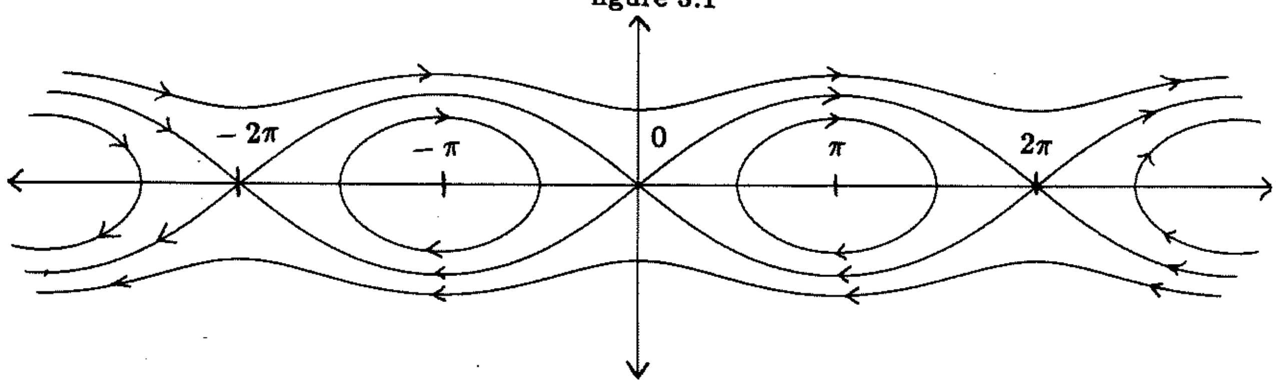

We have fixed points at $(2\pi N, 0)$ that satisfy the conditions for Melnikov's method. Consider the upper trajectory $(x_0(t), y_0(t))$ from $(0,0)$ to $(2\pi, 0)$. Along this trajectory we have x_0 satisfying the equation:

$$\dot{x}_0 = \frac{a\sqrt{\left(\frac{a}{\sqrt{a^2-1}} + 1 - \cos x_0\right)^2 \left(\frac{a^2-1}{a^2}\right) - 1}}{a + \sqrt{a^2 - 1}}.$$

This implicitly defines x_0 by

$$t = \int_{\pi}^{x_0} \frac{(a + \sqrt{a^2 - 1})dx}{a\sqrt{(\frac{a^2-1}{a^2})(\cos x - \frac{a}{\sqrt{a^2-1}} - 1)^2 - 1)}}.$$

By changing variables to $s = 1 - \cos x$, this integral becomes

$$\int_2^{1-\cos x_0} \frac{\frac{a^2}{\sqrt{a^2-1}} + a}{s\sqrt{(s + \frac{2a}{\sqrt{a^2-1}})(2-s)}} ds.$$

This can be solved exactly to yield:

$$\cos x_0 = 1 - \left(\frac{8a}{a + \sqrt{a^2 - 1}}\right)\left(\frac{1}{e^{\gamma t} + \beta + e^{-\gamma t}}\right),$$

$$\gamma = \left(\frac{\sqrt{a^2-1}}{a + \sqrt{a^2-1}}\right)\sqrt{\frac{4a}{\sqrt{a^2-1}}}, \quad \beta = 2\frac{a - \sqrt{a^2-1}}{a + \sqrt{a^2-1}}$$

along the upper saddle connection from $(0,0)$ to $(2\pi, 0)$.

3.1 Periodic Stretching of the Cat's Eye Flow

Instead of examining a general perturbation $g(\vec{x}, t)$, consider a perturbation of the parameter a. If we take a to be a time varying parameter of the form $a_0 + \varepsilon b(t)$, where $b(t)$ is periodic with period T, we get a phase diagram where the "cat's eyes" are periodically stretched and compressed by an ε amount. This corresponds to a time dependent solution to the Euler equation with external force.

To first order in ε, our perturbed equation is:

$$\dot{x} = \frac{a_0 \sinh y}{a_0 \cosh y + \sqrt{a_0^2 - 1}\cos x} - \frac{\varepsilon b(t) \sinh y \cos x}{\sqrt{a_0^2 - 1}(a_0 \cosh y + \sqrt{a_0^2 - 1}\cos x)^2}$$

$$\dot{y} = \frac{\sqrt{a_0^2 - 1}\sin x}{a_0 \cosh y + \sqrt{a_0^2 - 1}\cos x} + \frac{\varepsilon b(t) \sin x \cosh y}{\sqrt{a_0^2 - 1}(a_0 \cosh y + \sqrt{a_0^2 - 1}\cos x)^2}$$

The driving force for our perturbation is thus

$$\vec{F}_\varepsilon = \frac{\varepsilon b'(t)}{\sqrt{a^2-1}} e^{-2H_0(x,y)} \begin{pmatrix} -\sinh y \cos x \\ \sin x \cosh y \end{pmatrix}.$$

The perturbed Hamiltonian for this system is:

$$H = H_0 + \frac{\varepsilon b(t)}{\sqrt{a_0^2-1}} \left(\frac{\sqrt{a_0^2-1}\cosh y + a_0 \cos x}{a_0 \cosh y + \sqrt{a_0^2-1}\cos x} \right)$$
$$= H_0 + H_1.$$

Along all streamlines of the unperturbed flow,

$$H_1 \propto b(t)(\sqrt{a_0^2-1}\cosh y + a_0 \cos x).$$

Since the saddle connections are streamlines of the unperturbed flow, how they break up under a perturbation depends only on the perturbation at the points of the saddle connection. Thus, the Melnikov function for the above perturbation is identical to the one corresponding to the simpler perturbation:

$$H_1 = \varepsilon b(t)(\sqrt{a^2-1}\cosh y + a\cos x).$$

If we let $b(t)$ have the form $\cos(kt)$, then this perturbation corresponds to the superposition of four waves:

$$\sqrt{a^2-1}\cosh y(e^{i(z-kt)} + e^{i(z+kt)}) + a(e^{i(x-kt)} + e^{i(x+kt)}).$$

Here z is the third coordinate and we take the cross-sectional flow in the plane $z = 0$. The wavelength of the perturbation is exactly equal to the length of one of the Cat's Eyes. The wave speed is allowed to vary.

3.2 Properties of the Melnikov Function for Periodic Stretching

Consider the upper trajectory $(x_0(t), y_0(t))$ from $(0,0)$ to $(2\pi, 0)$ for the unperturbed system.

The Melnikov function for this trajectory is

$$M(t_0) = \int_{-\infty}^{\infty} C_1 \Bigg[\Bigg(a_0 \sin x_0(t) \cosh y_0(t) \sinh y_0(t) + \sqrt{a_0^2 - 1} \sinh y_0(t) \cos x_0(t) \sin x_0(t)) b(t + t_0) \Bigg) \Bigg] dt,$$

$$C_1 = \frac{1}{\sqrt{a_0^2 - 1}} \left(\frac{1}{(a_0 + \sqrt{a_0^2 - 1})^3} \right).$$

Which can be reduced to

$$M(t_0) = \int_{-\infty}^{\infty} C_2 (\sin x_0(t) \sinh y_0(t) b(t + t_0)) dt$$

where

$$C_2 = \frac{1}{\sqrt{a_0^2 - 1}(a_0 + \sqrt{a_0^2 - 1})^2}.$$

Here we have exploited the fact that

$$a_0 \cosh y_0(t) + \sqrt{a_0^2 - 1} \cos x_0(t) = a_0 + \sqrt{a_0^2 - 1}.$$

Claim. *$M(t_0)$ is well defined.*

Note that

$$\begin{aligned}
&\int_{-\infty}^{\infty} |(\sin x_0(t)) \sinh y_0(t)| dt \\
&= 2 \int_{-\infty}^{0} \sin x_0(t) \sinh y_0(t) dt \\
&= \frac{2(a_0 + \sqrt{a_0^2 - 1})}{\sqrt{a_0^2 - 1}} \int_{-\infty}^{0} \dot{y}_0(t) \sinh y_0(t) dt \\
&= \frac{2(a_0 + \sqrt{a_0^2 - 1})}{\sqrt{a_0^2 - 1}} [\cosh y(t)] \Big|_{-\infty}^{0} \\
&= \frac{4(a_0 + \sqrt{a_0^2 - 1})}{a_0} < \infty.
\end{aligned}$$

Thus $M(t_0)$ is a convergent integral.

Claim. $\int_0^T M(t_0) = 0$.

This is due to the fact that $M(t_0)$ is a convolution with an odd kernel. We have:

$$\int_0^T M(t_0)dt_0 = \int_0^T \int_{-\infty}^{\infty} C_2 \sin x_o(t) \sinh y_0(t) b(t+t_0) dt dt_0.$$

Since $b(t)$ is bounded, we can use Fubini's theorem to interchange the order of integration:

$$= \int_{-\infty}^{\infty} C_2 \sin x_0(t) \sinh y_0(t) \int_0^T b(t+t_0) dt_0 dt$$
$$= \int_{-\infty}^{\infty} C_2 \sin x_0(t) \sinh y_0(t) B dt.$$

Where $B = \int_0^T b(t)dt$. By simply examining the phase portrait, we see that $\sin x_0(t), \sinh y_0(t)$ are respectively odd and even functions of t. The above integral is thus zero. Similar results yield $\int_0^T M(t_0) = 0$ for all other saddle connections in this system. Since $M(t_0)$ has mean value zero, we expect that it will have simple zeros for a large class of perturbing functions $b(t)$.

Consider the case where $b(t) = \cos(kt)$. The above Melnikov integral then becomes

$$\int_{-\infty}^{\infty} C_2 \sin x_0(t) \sinh y_0(t) \cos k(t+t_0) dt$$
$$= -\sin(t_0) \int_{-\infty}^{\infty} C_2 \sin x_0(t) \sinh y_0(t) \sin(kt) dt$$
$$= -\sin(t_0) M_0(k),$$

where we define

$$M_0(k) = \int_{-\infty}^{\infty} C_3 \frac{d}{dt}[\cos x_0(t)] \sin(kt) dt,$$
$$C_3 = -(a_0 + \sqrt{a_0^2 - 1}) C_2.$$

Thus,

$$M_0(k) = \int_{-\infty}^{\infty} C_4 \frac{e^{\gamma t} - e^{-\gamma t}}{(e^{\gamma t} + \beta_0 + e^{-\gamma t})^2} \sin(kt) dt,$$
$$C_4 = C_3 \big(\gamma \big(\frac{8a_0}{a_0 + \sqrt{a_0^2 - 1}}\big)\big).$$

Evaluation by residues (see Appendix) yields, for $k \neq 0$, $(\frac{\gamma}{2\pi C_4})M_0(k) =$

$$\left[\frac{e^{-|m|\alpha}m}{2\sin\alpha} - \left(\frac{e^{-|m|2\pi}}{1-e^{-|m|2\pi}}\right)\left(\frac{m\sinh m\alpha}{\sin\alpha}\right)\right],$$

$$m = \frac{k}{\gamma}, \quad \alpha = \cos^{-1}(\beta_0/2).$$

Thus, $M_0(k)$ is non-zero almost everywhere. $M(t_0)$ has simple zeros for almost all k. A similar analysis shows that the lower trajectory has $M(t_0) = \sin(t_0)M_0(k)$ so that this trajectory will break up when the upper one does. Since both trajectories break up to yield transverse intersection of stable and unstable manifolds, we have satisfied the requirements for the heteroclinic theorem (Theorem 1.3.1) with N=2. Our perturbed system has a chaotic subsystem topologically equivalent to a shift on two symbols.

3.3 Mixing in the perturbed Cat's Eye Flow

By exploiting the symmetry of this model, we see that this perturbing function breaks up all trajectories transversely. In fact, we can view both the perturbed and unperturbed cases as flows on the cylinder. Here we take $x \in \mathbb{R}/2\pi, \quad y \in \mathbb{R}$. All of the saddle points are identified and we obtain two homoclinic orbits to a single saddle point. We can now use the standard homoclinic theorem to find a shift on two symbols.

Based on the proof of the theorem from the first section, we expect mixing to occur at least within the region around the fixed point. We know that there exists a neighborhood U of the fixed point $(0, 2\pi N)$ on which the Poincaré map for this system acts like a version of the horseshoe map. Qualitatively, we might expect such a mixing pattern to occur:

figure 3.2a

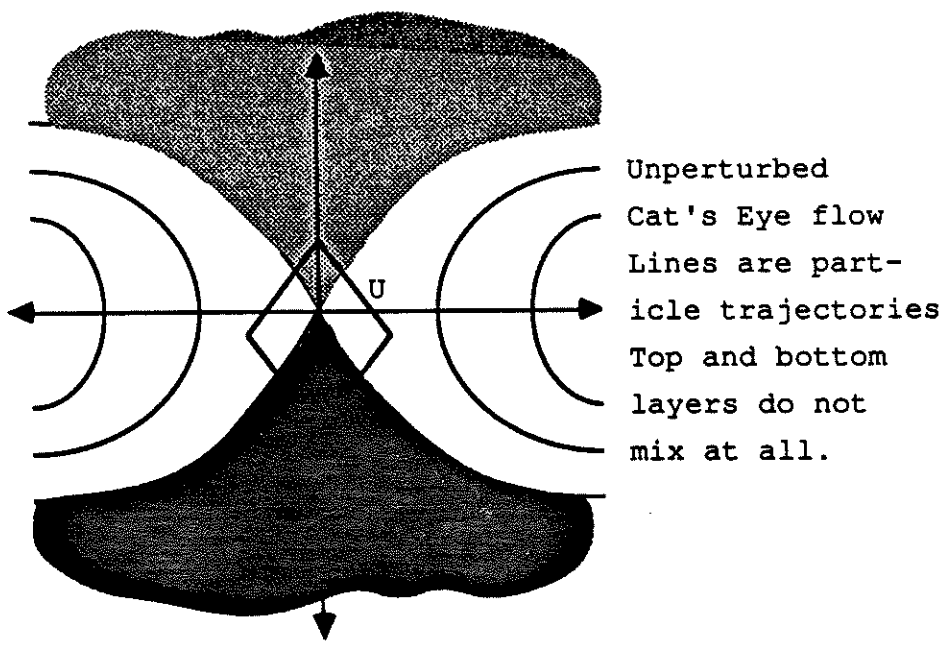

figure 3.2b

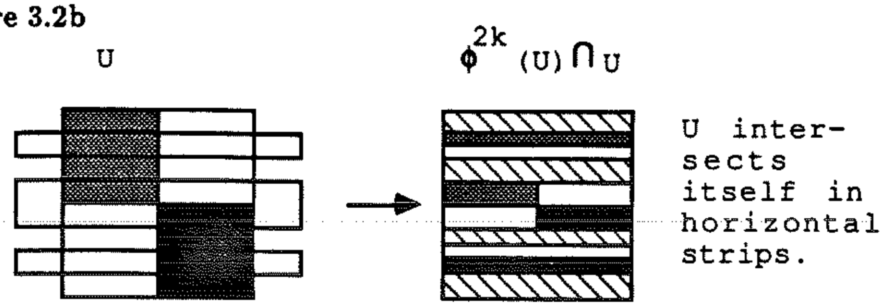

Perturbed Cat's Eye flow:
Here we see that that the top and bottom layers are mixed into the cat's eyes region and eventually into each other.

Viewed as a flow on the plane, we see that the perturbed system has the same geometric structure as the perturbed sine-Gordon equation. (Holmes [1981], section 3) The perturbed Cat's eye flow has a subsystem isomorphic to the shift on the symbols "+" and "–", where the "+" corresponds to traveling 'downstream' along an upper trajectory and the "–" corresponds to traveling 'upstream' along a lower trajectory (see fig 3.3). In the spirit of figure 3.2, this provides a mechanism for fluid inside one cat's eye to travel both upstream and downstream. This mechanism does not exist for the unperturbed case, since flow within an 'eye' will remain there for all time.

figure 3.3

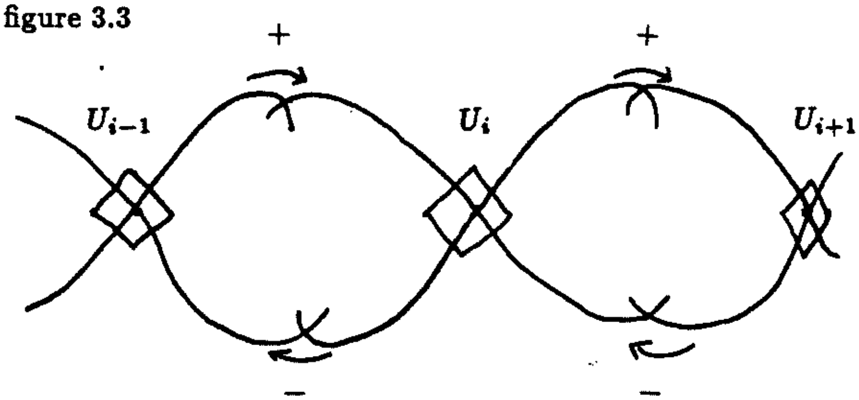

In the perturbed system, all saddle connections are broken up to give us transversal intersection of stable and unstable manifolds. The heteroclinic theorem tells us that at each fixed point $p_n = (2\pi n, 0)$, there is a neighborhood U_n, a unit square in local coordinates, such that for some fixed time T^*, the flow φ_{T^*} maps U_i to intersect U_{i-1} and U_{i+1} in horizontal strips. A simplified model of the dynamics present is pictured in fig. 3.4.

figure 3.4

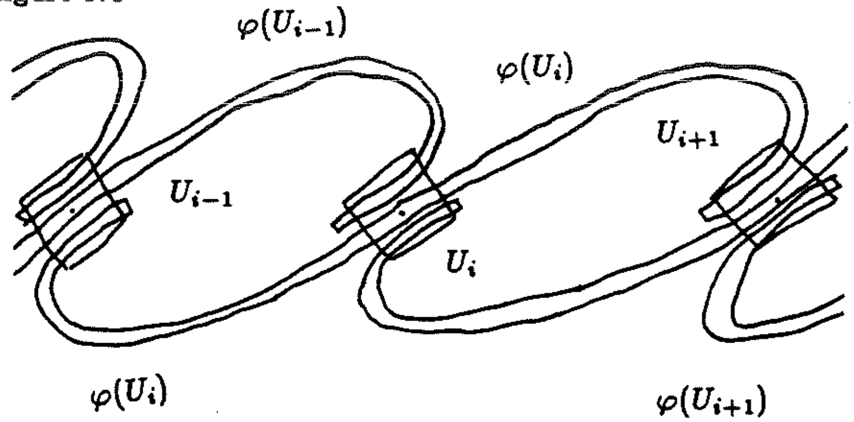

Here each U_i is intersected by the horizontal strips $H_{i-1,i} = \varphi(U_{i-1}) \cap U_i$ and $H_{i+1,i} = \varphi(U_{i+1}) \cap U_i$.

By the symmetry of the flow and its perturbation, we can choose each U_i so that $U_i + 2\pi = U_{i+1}$ and $\varphi(U_i) + 2\pi = \varphi(U_{i+1})$. Our invariant set is

$$I = \bigcap_{k=-\infty}^{\infty} \varphi^{-k}\Big(\bigcup_i (H_{i+1,i} \cup H_{i-1,i})\Big).$$

I can be decomposed into disjoint sets $I_i = U_i \cap I$. For any given i, we have a one-to-one correspondence between I_i and $S^{\pm}$, the set of all bi-infinite sequences of "+" and "−":

$$\tau : I_i \longrightarrow S^{\pm}$$
$$\begin{aligned} [\tau(x)]_l = &\quad + \quad \text{if} \quad \varphi^l(x) \in U_k \Rightarrow \varphi^{l+1}(x) \in U_{k+1} \\ = &\quad - \quad \text{if} \quad \varphi^l(x) \in U_k \Rightarrow \varphi^{l+1}(x) \in U_{k-1}. \end{aligned}$$

Thus there is a set $S^{\pm}$ of sequences corresponding to each I_i. We see that there is a mechanism for pieces of fluid to move rather chaotically both upstream and downstream as well as for fluid within each 'eye' to mix with fluid in other 'eyes'.

This mixing and chaotic motion was not present in the unperturbed Cat's Eye flow. The fact that this perturbation leads to such chaos for almost all k indicates that such mixing may be rather common in the actual shear layers.

4 Planar Lattice Flow

We consider the following flow:

$$\dot{x}_1 = -\sin(2\pi x_1)\sin(2\pi x_2)$$
$$\dot{x}_2 = -\cos(2\pi x_1)\cos(2\pi x_2)$$

a Hamiltonian system with $H_0 = (2\pi)^{-1}\sin(2\pi x_1)\cos(2\pi x_2)$. This is a model for axisymmetric Taylor vortex flow as well as for many convective flows (see Van Dyke [1982], p. 76, 82 for photographs of these flows). If we take x_1 to be a moving coordinate, these equations model the Rossby waves of geophysical fluid dynamics (see Pedlosky [1982], p. 84).

figure 4.1

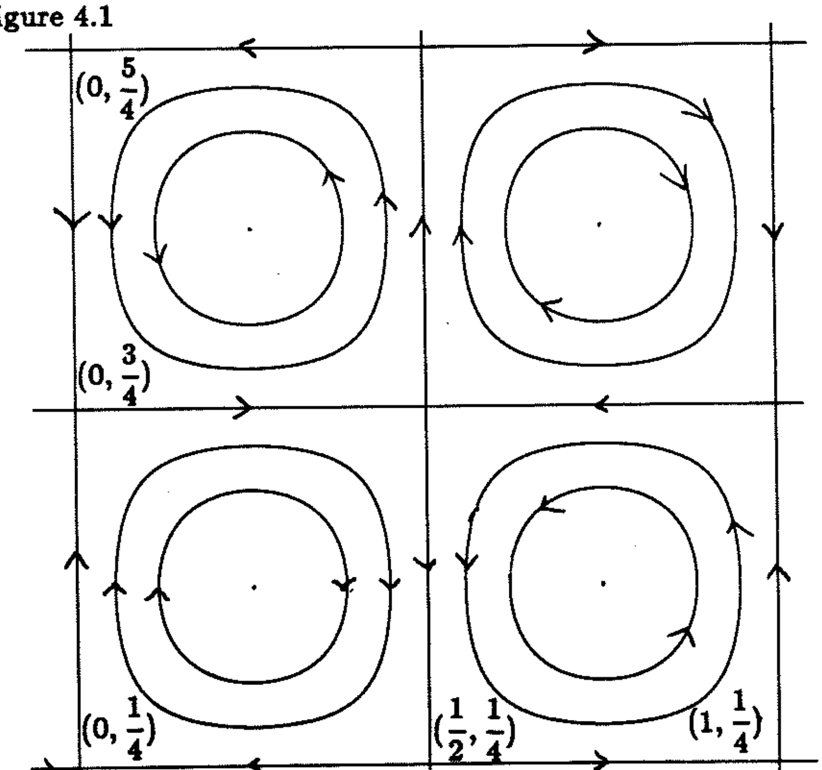

This flow is obviously doubly periodic, yielding a flow on the torus $T = \mathbb{R}^2/\Gamma$ where Γ is the lattice $\{(n_1, n_2); n_1, n_2 \in \mathbb{Z}\}$.

Viewed as a flow on the torus T, we obtain a system with heteroclinic orbits connecting four saddle points. Melnikov's theory can then be applied to perturbations of this flow.

We can also map this flow onto a "smaller" torus $T' = \mathbb{R}^2/\Gamma'$ where $\Gamma' = \{(1/2(n_1 - n_2), 1/2(n_1 + n_2))\}$. Here we have exploited the periodicity in the variables $(x_1 - x_2), (x_1 + x_2)$ as well as in x_1 and x_2. The flow on T' has only two heteroclinic saddle points. By examining perturbed flows on T', we can look for a subsystem that is a shift on two symbols. This horseshoe like structure will result if all heteroclinic orbits are broken up so that stable and unstable manifolds intersect transversely.

4.1 Time and Space Dependent Perturbations

We consider two types of perturbations, ones that are functions of time only and ones that have an added space dependence. In the purely time dependent case, we have $\varepsilon \vec{f}(t)$ as a perturbation to the velocity field, with $f_i(t) = f_i(t + T)$ for $i = 1, 2$. This corresponds to an external driving force $\vec{F}_\varepsilon = \varepsilon \vec{f}'(t)$ which is uniform in space at any given moment. This is physically reasonable as an approximation to an external force which is time periodic and has an average space variation much larger than the periodic lattice structure of the flow. For the vertical saddle connections, the Melnikov function for this perturbation is

$$M_v(t_0) = \pm \int_{-\infty}^{\infty} \cos(2\pi x_2(t)) f_1(t + t_0) dt$$

since $\sin(2\pi x_1) = 0$ for these trajectories. Likewise for the horizontal orbits, $\cos(2\pi x_2) = 0$ and so

$$M_h(t_0) = \pm \int_{-\infty}^{\infty} \sin(2\pi x_1(t)) f_2(t + t_0) dt$$

We see that the vertical and horizontal components of $\vec{f}$ are decoupled. We shall show by symmetry properties that f_1 and f_2 must satisfy the same conditions in order for M_v and M_h to have simple zeros. For this space-independent perturbation, the Γ'-lattice symmetry is preserved and chaotic motion can be reduced to a subsystem isomorphic to the shift on two symbols. The following example presents a spatially dependent perturbation that breaks up the Γ' symmetry.

In general, a perturbing velocity of the form

$$\varepsilon \begin{pmatrix} v_1(x_2, t) \\ v_2(x_1, t) \end{pmatrix}$$

constitutes a solution to the two dimensional Euler equation with external force

$$\vec{F}_\varepsilon = \varepsilon \begin{pmatrix} \partial v_1(x_2, t)/\partial t \\ \partial v_2(x_1, t)/\partial t \end{pmatrix}.$$

A particularly interesting perturbation of this form is

$$\varepsilon \begin{pmatrix} v_1 \\ v_2 \end{pmatrix} = \varepsilon \begin{pmatrix} \cos(2\pi x_2) \cos kt \\ \sin(2\pi x_1) \cos kt \end{pmatrix}.$$

This has a stream function

$$\frac{\varepsilon}{2\pi} \cos kt[\sin(2\pi x_2) - \cos(2\pi x_1)],$$

which can be viewed as a superposition of linear waves traveling along coordinate axes:

$$-(e^{i(2\pi x_1 + kt)} + e^{i(2\pi x_1 - kt)}) - i(e^{i(2\pi x_2 + kt)} - e^{i(2\pi x_2 - kt)}).$$

This perturbation is geometrically interesting because it breaks up the Γ' symmetry and we are forced to consider heteroclinic orbits joining four points instead of two points. We shall show that for almost all k, the saddle connections breaks up to yield a subsystem topologically equivalent to the shift on four consecutive symbols.

4.2 Explicit Calculation of the Melnikov Functions

Along an unperturbed horizontal saddle connection, we have

$$\dot{x}_1 = \pm \sin(2\pi x_1), \quad \dot{x}_2 = 0$$

and along a vertical connection

$$\dot{x}_2 = \pm \cos(2\pi x_2), \quad \dot{x}_1 = 0.$$

In the case of the connection from $(\frac{1}{2}, \frac{1}{4})$ to $(0, \frac{1}{4})$, we have $\dot{x}_1 = -\sin(2\pi x_1)$. This has a solution $x_1 = \frac{1}{\pi}\tan^{-1}(e^{-2\pi t})$ which by symmetry properties of the flow yields

$$\sin(2\pi x_1) = \pm\frac{2e^{-2\pi t}}{1+e^{-4\pi t}}$$

along all horizontal connections and

$$\cos(2\pi x_2) = \pm\frac{2e^{-2\pi t}}{1+e^{-4\pi t}}$$

along all vertical ones.

For a spatially independent perturbation, the Melnikov function of section 4.1, for either saddle connection, is of the form

$$M_i(t_0) = \int_{-\infty}^{\infty} \frac{2e^{-2\pi t}}{1+e^{-4\pi t}} f_i(t+t_0)dt.$$

If we expand f_i into its Fourier series,

$$f_i(t) = \sum_{k=-\infty}^{\infty} (A_k \cos(2\pi kt/T) + B_k \sin(2\pi kt/T))$$

we find that $M_i(t_0) =$

$$\sum_{k=-\infty}^{\infty} \left[(A_k \cos(2\pi kt_0/T) + B_k \sin(2\pi kt_0/T)) \int_{-\infty}^{\infty} \frac{2e^{-2\pi t}}{1+e^{-4\pi t}} \cos(2\pi kt/T)dt \right].$$

Evaluation by residues reveals

$$M_i(t_0) = \sum_{k=-\infty}^{\infty} (A_k \cos(2\pi k t_0/T) + B_k \sin(2\pi k t_0/T))(\frac{1}{e^{-\pi k/2T} + e^{\pi k/2T}}).$$

Whether or not $M_i(t_0)$ has simple zeros depends on the respective values of A_k and B_k. For example, if $f_i = A_0 + A_1 \cos(2\pi k t/T)$, we require

$$|A_0| < |A_1| \left[\frac{2}{e^{-\pi k/2T} + e^{\pi k/2T}} \right]$$

for $M_i(t_0)$ to have simple zeros. We see now that the class of perturbing functions $\vec{f} = (A\cos(t), B\sin(t))$ yields $M_v(t_0)$ and $M_h(t_0)$ with simple zeros for all saddle connections. Applying the results of the first section yields a shift on four symbols as a subsystem of the perturbed flow on T, and a shift on two symbols as a subsystem of the perturbed flow on T'.

For the spatially dependent perturbation

$$\varepsilon \begin{pmatrix} \cos(2\pi x_2) \cos kt \\ \sin(2\pi x_1) \cos kt \end{pmatrix}$$

we find that, up to a change of sign, the Melnikov function for either a vertical or horizontal saddle connection is

$$M(t_0) = 4\cos(kt_0) \int_{-\infty}^{\infty} \frac{e^{-4\pi t}}{(1 + e^{-4\pi t})^2} \cos kt dt.$$

which we evaluate via residues to be

$$\begin{aligned} M(t_0) &= \cos kt_0 \left(\frac{k}{4\pi \sinh(k/4)} \right) \\ &= \cos kt_0 M_0(k). \end{aligned}$$

$M_0(k)$ is nonzero for almost all k so that the Melnikov function will have simple zeros and we have a subsystem topologically equivalent to the shift on four consecutive symbols.

4.3 Mixing in the Perturbed Lattice Flow

Under both perturbations, we expect some sort of mixing to occur that was not present in the unperturbed case. In the perturbed systems, all connections are broken up to yield transversal intersection of stable and unstable manifolds. As in the cat's eye model, at each fixed point $p_{n_1 n_2} = (\frac{1}{2}n_1, \frac{1}{2}n_2 + \frac{1}{4}), \quad n_1, n_2 \in \mathbb{Z}$, we have neighborhoods $U_{n_1 n_2}$ that intersect each other in horizontal strips under some fixed time mapping of the flow (see fig 4.2).

figure 4.2

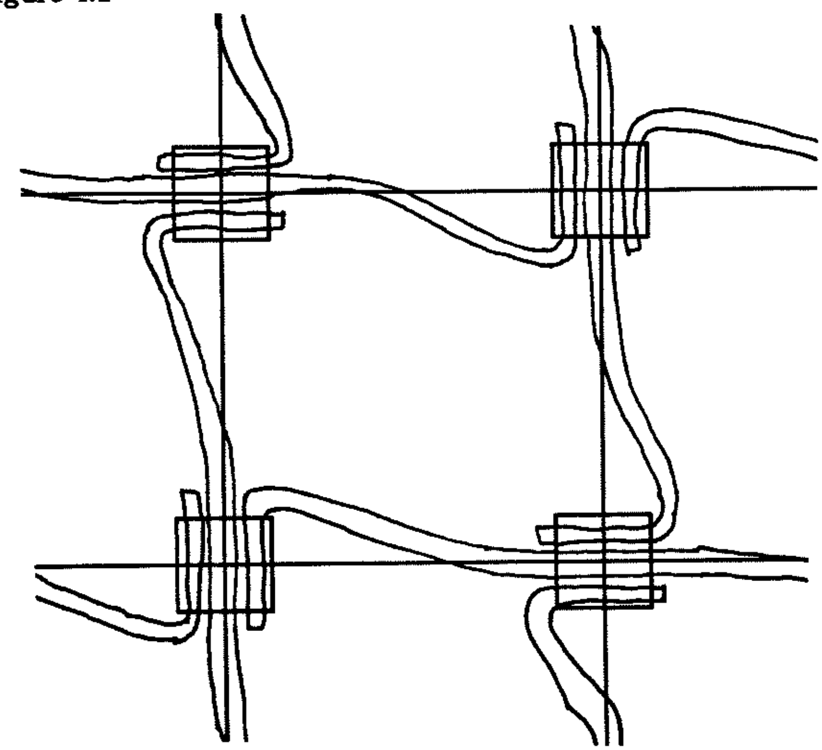

In the case of the first perturbation studied, we can exploit the T' symmetry to obtain a subsystem topologically equivalent to the shift on two symbols. The perturbed and unperturbed systems are both flow on the torus T'. Under this symmetry, we can identify all clockwise rotating cells with each other and likewise all counter clockwise rotating cells with each other. In the unperturbed case, these patches of fluid do not mix. The perturbation satisfies the conditions of the heteroclinic theorem with two fixed points, yielding a subsystem of the flow topologically equivalent to the shift on two symbols. In the perturbed case we see mixing patterns similar to those present in the Cat's Eye flow (see fig. 4.3).

In the case of the second perturbation, we do not have the T' symmetry. The cells break up into two different clockwise and counterclockwise rotations(see fig. 4.4). On the torus T we have four fixed points in the heteroclinic orbit and our system breaks up to yield a subsystem topologically equivalent to the shift on four consecutive symbols. In the previous case we have symbols 1 and 2 identified with 3 and 4. This is analogous to identifying the two clockwise rotations with each other and likewise the two counter clockwise rotations with each other. Again we expect similar mixing patterns to occur. (see fig. 4.5).

figure 4.3a

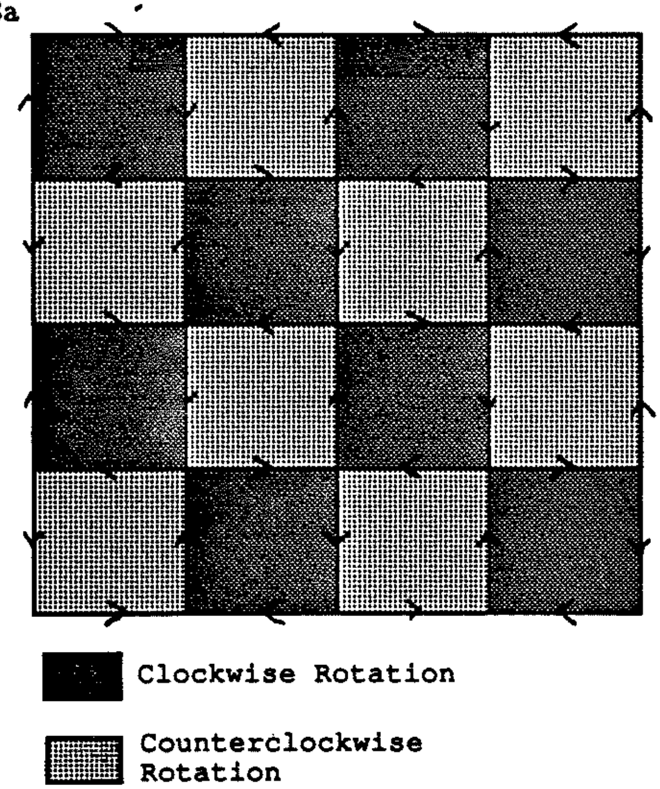

figure 4.3b

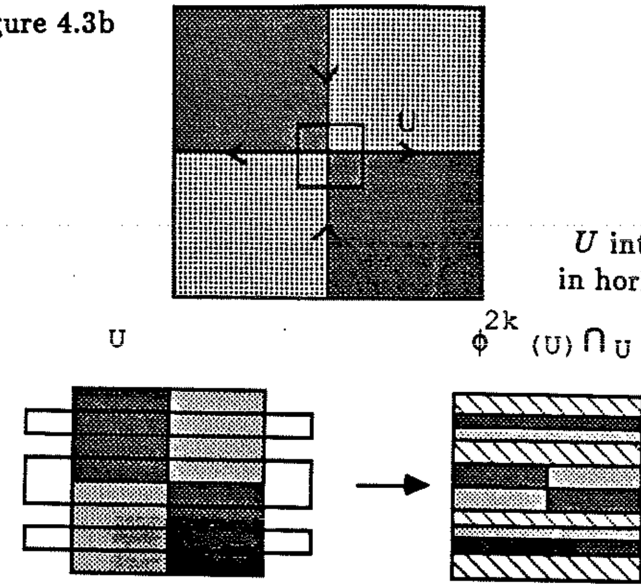

U intersects itself in horizontal strips.

Different flow regions are mixed together in a neighborhood of *U*.

figure 4.4

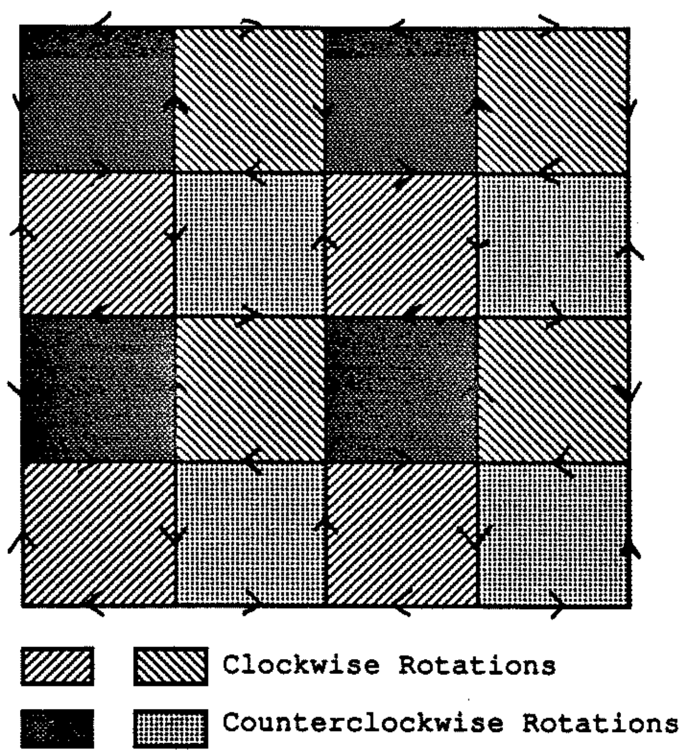

figure 4.5

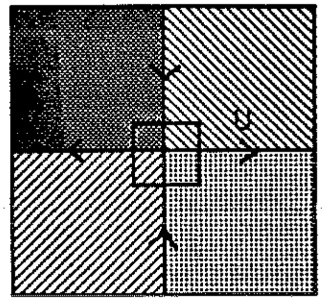

Again, U intersects itself in horizontal strips.

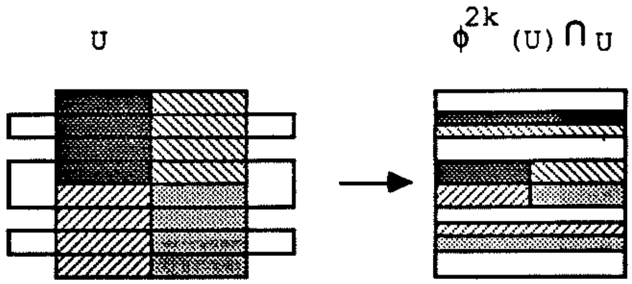

Different flow regions are mixed together in a neighborhood of U.

5 Motion of an Elliptical Vortex in a Strain Field

An important part of fluid mechanics is the study of vortices, their structure, and how they interact with one another. In chapters three and four we examined two well known two dimensional planar fluid models. Since organized vortex structures are observed frequently, we would like to find a simple model for a vortex affected by a field of neighboring vortices. As the examples of chapters three and four indicate, the presence of multiple vortices in stationary planar fluid flow often results in fixed points of the flow, between vortex structures, that can be modeled as hyperbolic saddle points in a planar dynamical system. In a neighborhood of such saddle points, the velocity field is roughly linear and can be locally approximated by a simple strain. It is thus physically reasonable to model certain vortex interaction locally as a single vortex in a straining flow. Moore and Saffman [1975], as well as Neu [1984], describe vortex interaction that can be modeled in such a way.

We study the motion of an elliptical vortex in a three dimensional imposed strain. We see that the evolution of such a vortex can be characterized as a planar dynamical system that has interesting Hamiltonian and non-Hamiltonian formulations involving the aspect ratio $\eta = a/b$ and the angle θ of rotation of the ellipse. Here a and b correspond to the major and minor axes of the ellipse. We apply Melnikov's method to the evolution equations of the vortex to show chaotic dynamics occurring in the presence of three dimensional periodic stretching of the imposed strain. The actual analysis differs somewhat from what was done in the previous sections in that we study chaos occurring in the evolution equation of the shape and orientation of the ellipse as opposed to chaos occurring in the flow pattern of an actual fluid model.

5.1 Hamiltonian formulation of Exact Euler Solution

The Hamiltonian formulation presented below is due to Neu [1984] and represents a three dimensional generalization of the exact solutions of an elliptical vortex in a two dimensional straining flow (described by Kida [1981]). First consider a planar vortex region in the shape of an ellipse with constant vorticity in the interior. The points on the boundary of the region are solutions to the equation $\frac{x^2}{a^2} + \frac{y^2}{b^2} = \text{constant}$. Following a potential theory calculation described in Lamb's *Hydrodynamics* [1945], we see that the velocity field inside the ellipse is linear:

$$\begin{pmatrix} \dot{x} \\ \dot{y} \end{pmatrix} = \tilde{U}(a,b,\theta) \begin{pmatrix} x \\ y \end{pmatrix},$$

$$\tilde{U}(a,b,\theta) = -\frac{\omega}{a+b} R(\theta) \begin{pmatrix} 0 & a \\ -b & 0 \end{pmatrix} R(\theta).$$

Here a and b correspond to the major and minor axes of this elliptical cross section and θ is the angle of the major axis with respect to the x-axis. $R(\theta)$ is the rotation matrix $\begin{pmatrix} \cos\theta & -\sin\theta \\ \sin\theta & \cos\theta \end{pmatrix}$.

In three dimensions we have a cylindrical vortex region whose cross section in the xy-plane is the above velocity field. We add an irrotational straining field whose velocity is given by $v = (\gamma' x, -\gamma y, \gamma'' z)$ where $\gamma' - \gamma + \gamma'' = 0$ is required for incompressibility. The combination of vortex and strain yields a fluid velocity which in the xy-plane has the form $U(a,b,\theta)(x,y)^T$ where

$$U(a,b,\theta) = -\frac{\omega}{a+b} R(\theta) \begin{pmatrix} 0 & a \\ -b & 0 \end{pmatrix} R(\theta) + \begin{pmatrix} \gamma' & 0 \\ 0 & -\gamma \end{pmatrix}.$$

The velocity field inside the vortex is again linear and the path of a fluid particle on the boundary must satisfy the equation of an ellipse which we write in matrix form:

$$\begin{pmatrix} x \\ y \end{pmatrix} E(a,b,\theta) \begin{pmatrix} x & y \end{pmatrix} = \text{constant},$$

$$E(a,b,\theta) = R(\theta) \begin{pmatrix} a^{-2} & 0 \\ 0 & b^{-2} \end{pmatrix} R(\theta).$$

Differentiating the ellipse equation yields

$$\dot{X}^T E X + X^T \dot{E} X + X^T E \dot{X} = 0$$

where X is the vector (x, y). Since $\dot{X} = U(a, b, \theta)X$, we have the matrix evolution equation,

$$\dot{E} + U^T E + EU = 0$$

which we can write out explicitly in terms of a, b, and θ to give us the evolution equations for the elliptical vortex:

$$\dot{a} + (\gamma \sin^2 \theta - \gamma' \cos^2 \theta)a = 0,$$

$$\dot{b} + (\gamma \cos^2 \theta - \gamma' \sin^2 \theta)b = 0,$$

$$\dot{\theta} = \frac{\omega ab}{(a+b)^2} - \frac{1}{2}(\gamma + \gamma')\frac{a^2 + b^2}{a^2 - b^2} \sin 2\theta.$$

These evolution equations have the following Hamiltonian formulation: let $\eta = \frac{a}{b}$ be the aspect ratio and τ be a dimensionless time defined by $\frac{d\tau}{dt} = \frac{\omega \eta^2}{\eta^2 - 1}$. Then the evolution equations become

$$\begin{aligned}
\frac{d\eta}{d\tau} &= -\frac{\partial H}{\partial \theta} = \frac{\gamma + \gamma'}{\omega}(\eta - \frac{1}{\eta}) \cos 2\theta \\
\frac{d\theta}{d\tau} &= \frac{\partial H}{\partial \eta} = \frac{\eta - 1}{\eta(1 + \eta)} - \frac{1}{2}\frac{\gamma + \gamma'}{\omega}(1 + \frac{1}{\eta^2}) \sin 2\theta \\
H &= \log \frac{(1 + \eta)^2}{\eta} - \frac{1}{2}\frac{\gamma + \gamma'}{\omega}(\eta - \frac{1}{\eta}) \sin 2\theta.
\end{aligned}$$

We consider γ,γ', and ω to be in general time dependent parameters in this equation. The total circulation of the vortex is $\Gamma = \pi ab\omega$ which we know to be constant, by the Kelvin circulation theorem (see p. 28, Chorin and Marsden [1979]). The evolution equations imply that

$$\frac{d(ab)}{dt} = (\gamma' - \gamma)ab$$

so that

$$ab = a_0 b_0 e^{(\gamma' - \gamma)t}$$

which in turn yields

$$\omega = \omega_0 e^{(\gamma - \gamma')t}.$$

Thus, when $\gamma'' = 0$, $\gamma' - \gamma + \gamma'' = 0$ implies that $\gamma = \gamma'$. Our Hamiltonian system is autonomous if and only if $\gamma'' = 0$, γ, γ' are both constant. We will consider the case where this autonomous Hamiltonian system is perturbed by a periodic stretching of the strain where we set $\gamma'' = \varepsilon g(t)$.

In the autonomous case, we have $\gamma = \gamma'$, and are interested in the dynamics indicated in the phase portrait for $0 < \gamma/\omega < 0.15$ (see fig. 5.1). There are no heteroclinic orbits in the phase portrait for $\gamma/\omega > .15$. The three interesting regimes are depicted in fig. 5.1:

(1) For $0 < \gamma/\omega < .1227$, there are oscillating regions (bubbles close to the $\log \eta = 0$ axis) as well as rotating regions between the bubbles and the outer saddle connections.

(2) At $\gamma/\omega = .1227$ we have a bifurcation where saddle connections between three fixed points exist for this value of γ/ω only.

(3) for γ/ω between .1227 and .15, we have homoclinic saddle connections, the interior of which represents an ellipse oscillating about the ray $\theta = \pi/4$.

The importance of the bifurcation is that in regimes (2) and (3) we no longer have the possibility of a rotating ellipse.

5.2 Real Time Formulation of Evolution Equations

In order to apply Melnikov's method to the above Hamiltonian system, we would need to consider time-periodic perturbations of the dimensionless time τ. This is not a reasonable physical model, since a periodic perturbation of the straining flow would be periodic in real time, not the dimensionless time τ. Note that the evolution equations written in terms of the orientation, aspect ratio and real time are:

$$\frac{d\theta}{dt} = \frac{\omega\eta}{(\eta+1)^2} - \frac{1}{2}(\gamma+\gamma')\frac{\eta^2+1}{\eta^2-1}\sin 2\theta$$

$$\frac{d\eta}{dt} = (\gamma+\gamma')\eta\cos 2\theta.$$

Since (η, θ) and $(\eta^{-1}, \theta+\pi/2)$ correspond to the same ellipse, we can paramatrize the evolution equation in terms of $r = \log\eta$, $\varphi = 2\theta$ yielding a polar coordinates formulation for these equations in which there is a one to one correspondence between ellipses and points in the phase space (r, φ). The evolution equations become:

$$\dot{r} = (\gamma+\gamma')\cos\varphi$$

$$\dot{\varphi} = \frac{2\omega e^r}{(e^r+1)^2} - (\gamma+\gamma')\frac{e^{2r}+1}{e^{2r}-1}\sin\varphi.$$

¿From the Hamiltonian formulation, we know that trajectories correspond to constants of

$$H = \log\left[\frac{(1+e^r)^2}{e^r}\right] - \frac{\gamma+\gamma'}{2\omega}(e^r - e^{-r})\sin\varphi.$$

This can be verified by calculating that $dH/dt = 0$ for the real time t. These equations seem to blow up for $r = 0$. Fortunately, we see that this blow up is due to the coordinates we are using and not the equations themselves. Polar coordinates are not well defined at $r = 0$ so we convert the equations to Cartesian form by $x = r\cos\varphi$, $y = r\sin\varphi$. The evolution equations become:

$$\dot{x} = (\gamma+\gamma')\frac{x^2}{x^2+y^2} - \frac{2\omega y e^{\sqrt{x^2+y^2}}}{(e^{\sqrt{x^2+y^2}}+1)^2} + (\gamma+\gamma')\frac{e^{2\sqrt{x^2+y^2}}+1}{e^{2\sqrt{x^2+y^2}}-1}\frac{y^2}{\sqrt{x^2+y^2}}$$

$$\dot{y} = (\gamma+\gamma')\frac{xy}{x^2+y^2} + \frac{2\omega x e^{\sqrt{x^2+y^2}}}{(e^{\sqrt{x^2+y^2}}+1)^2} - (\gamma+\gamma')\frac{e^{2\sqrt{x^2+y^2}}+1}{e^{2\sqrt{x^2+y^2}}-1}\frac{xy}{\sqrt{x^2+y^2}}.$$

We see that as $r \to 0$, the first and third terms in $\dot{x}$ appear to blow up. Using Taylor expansion techniques, we see that the third term can be approximated by

$$(\gamma + \gamma')\frac{y^2}{x^2 + y^2}(1 + \mathcal{O}(r^2))$$

for r small. Thus, $\dot{x} \to \gamma + \gamma'$ as $r \to 0$. In a similar fashion, we see that $\dot{y} \to 0$ as $r \to 0$.

The phase portrait (fig. 5.2) for the real time formulation has a much simpler form than the Hamiltonian one of the previous section. We see that for $(\gamma+\gamma')/2\omega <$ .15, there is a homoclinic loop with hyperbolic fixed point corresponding to the largest root of $e^r(e^r - 1) = ((\gamma+\gamma')/2\omega)(e^{2r}+1)(e^r+1)$. We see that the bifurcation at $\gamma/\omega = .1227$ is represented by the loop crossing the origin.

Figure 5.1

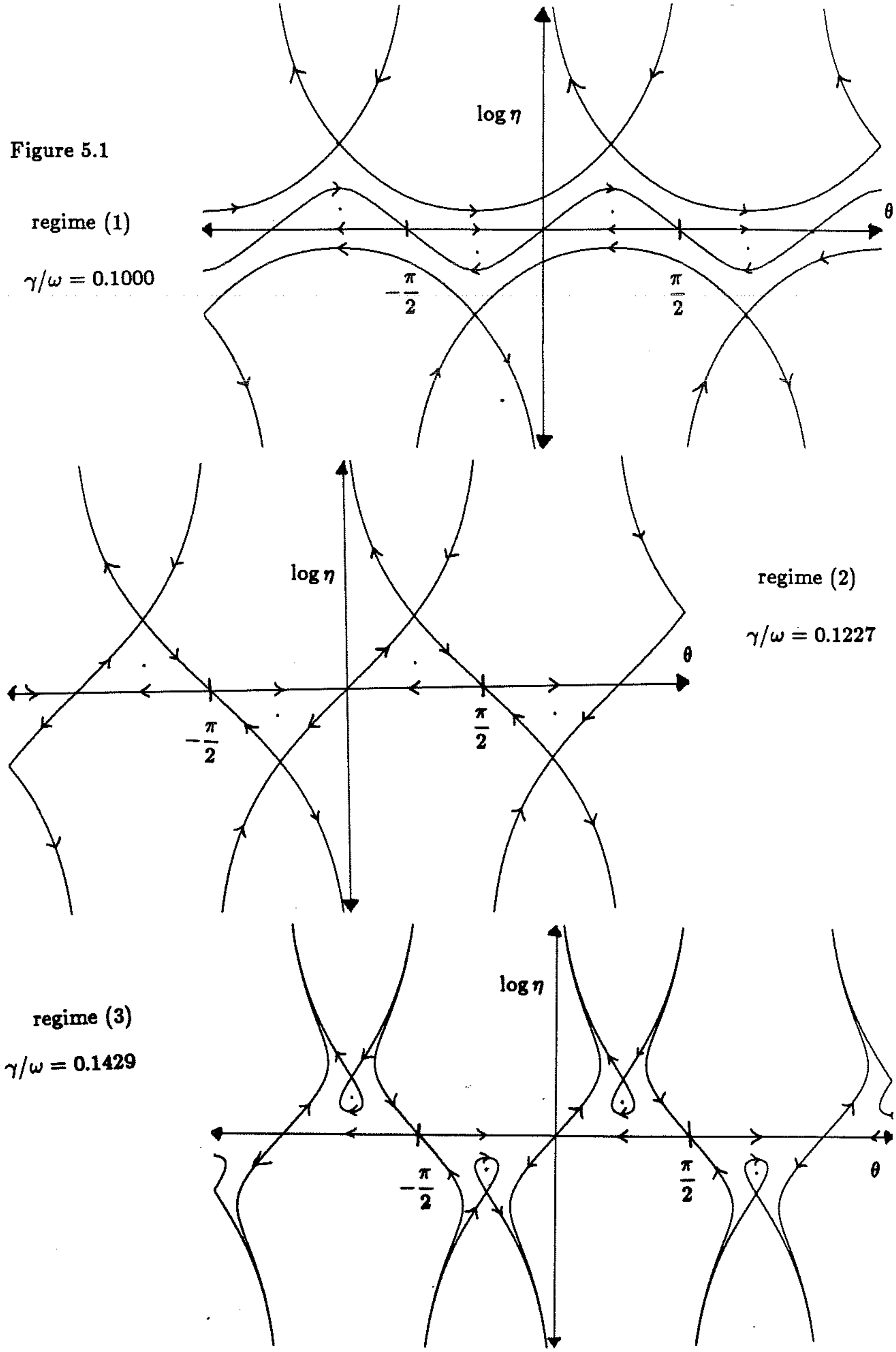
regime (1)
$\gamma/\omega = 0.1000$
$\log \eta$
θ
$-\frac{\pi}{2}$
$\frac{\pi}{2}$
regime (2)
$\gamma/\omega = 0.1227$
$\log \eta$
θ
$-\frac{\pi}{2}$
$\frac{\pi}{2}$
regime (3)
$\gamma/\omega = 0.1429$
$\log \eta$
θ
$-\frac{\pi}{2}$
$\frac{\pi}{2}$

Figure 5.2

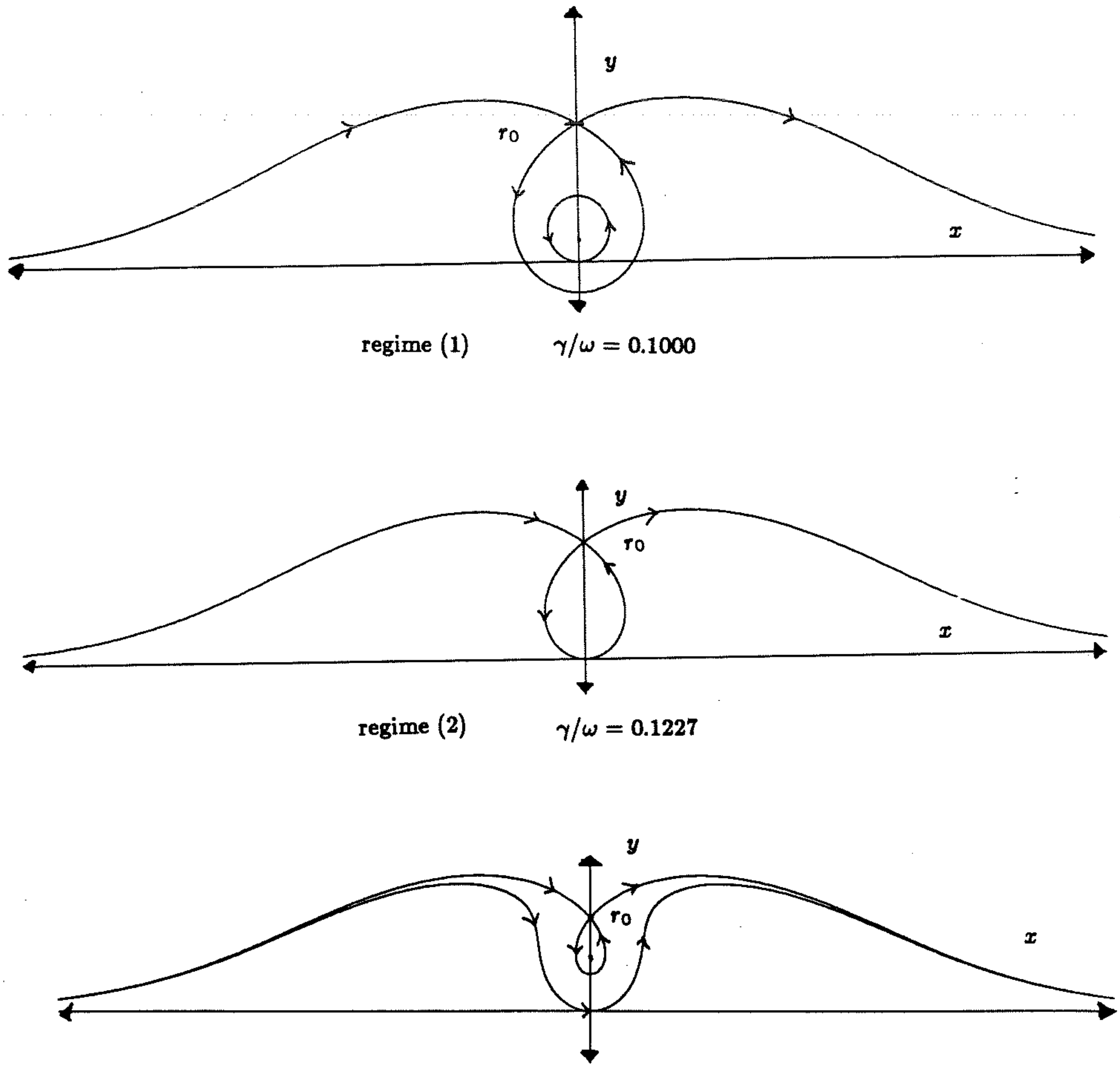

regime (1) $\gamma/\omega = 0.1000$

regime (2) $\gamma/\omega = 0.1227$

regime (3) $\gamma/\omega = 0.1429$

5.3 Periodic Stretching of an Elliptical Vortex

In general, our perturbed system will have the form

$$\dot{r} = C_0 \cos\varphi + \varepsilon g_1(r, \varphi, t)$$

$$\dot{\varphi} = \frac{2\omega_0 e^r}{(e^r+1)^2} - C_0 \frac{e^{2r}+1}{e^{2r}-1} \sin\varphi + \varepsilon g_2(r, \varphi, t).$$

Here g_1 and g_2 are periodic in time, $C_0 = (\gamma_0 + \gamma_0')$.

For $0 < C_0/\omega_0 < 0.15$, the unperturbed system has a hyperbolic fixed point p_0 at $\varphi = \pi/2, r = r_0$ where r_0 corresponds to the largest real root of the cubic $e^{3r} + e^{2r}(1-B) + e^r(1+B) + 1 = 0$ where $B = (\frac{1}{2}C_0\omega_0)^{-1}$. This fixed point has a homoclinic saddle connection Γ_0 as depicted in figure 5.2. If we consider a perturbation involving a periodic stretching by an amount $\varepsilon\gamma''(t)$, then our perturbation has the form

$$g_1 = C_1(t) \cos\varphi$$

$$g_2 = \frac{2C_2(t)e^r}{(e^r+1)^2} - C_1(t)\frac{e^{2r}+1}{e^{2r}-1} \sin\varphi.$$

Here C_1 and C_2 are periodic in time with period T. We consider the symmetric case where the oscillation of γ'' puts equal and opposite oscillations on γ' and γ while maintaining the incompressibility condition $\gamma' - \gamma + \gamma'' = 0$. Thus, $\gamma + \gamma'$ stays constant even though $\gamma - \gamma'$ oscillates with γ''. This implies that $C_1(t) = 0$ so that our perturbation has the simpler form

$$g_1 = 0,$$
$$g_2 = \frac{2C_2(t)e^r}{(e^r+1)^2}.$$

If we paramatrize Γ_0 by $(r(t), \varphi(t))$, the Melnikov function for the perturbed system can be calculated using the non-Hamiltonian form. There are two ways of doing the Melnikov function calculation. We can view Γ_0 as a trajectory in the (r, φ) coordinate system which has the advantage of a simpler formulation. Since these coordinates break up at $r = 0$, we can not treat the case where Γ_0 contains the point $r = 0$. This occurs only at the value $\gamma/\omega = .1227$. For any other value of γ/ω, we can find a C^∞ vector field $(f_1(r,\varphi), f_2(r,\varphi))$ so that

$$\dot{r} = f_1(r,\varphi)$$
$$\dot{\varphi} = f_2(r,\varphi)$$

is a planar differentiable dynamical system in the coordinates (r,φ) with a saddle connection identical to Γ_0 in its real time paramatrization. We have $f_1 = C_0 \cos\varphi$, $f_2 = 2\omega_0 e^r/(e^r+1)^2 - C_0 \sin\varphi(e^{2r}+1)/(e^{2r}-1)$ in a neighborhood of the curve Γ_0. This new dynamical system is suitable for Melnikov's method and in a neighborhood of Γ_0 has dynamics identical to that of the original system.

Alternatively, we can treat the evolution equation as a dynamical system in the (x,y) coordinates. This allows us to show that chaos will also occur in the degenerate case of $\gamma/\omega = .1227$. Both calculations are presented:

The Melnikov function in (r,φ) coordinates:

For this we need to know $\exp\left(\int_0^t trDf(\Gamma_0(s))ds\right)$. We have

$$trDf = -C_0 \frac{e^{2r}+1}{e^{2r}-1}\cos\varphi = \frac{-\dot{r}(e^{2r}+1)}{e^{2r}-1}.$$

This gives us

$$\exp\left(\int_0^t trDf(\Gamma_0(s))ds\right)\frac{e^{r(t)}(e^{r_0}-e^{-r_0})}{e^{2r(t)}-1}.$$

This yields a Melnikov function

$$M(t_0) = C_3 \int_{-\infty}^{\infty} \frac{e^{2r}\cos\varphi}{(e^r+1)^2(e^{2r}-1)} C_2(t+t_0)dt,$$

$$C_3 = C_0(e^{r_0} - e^{-r_0}).$$

Using the fact that the integral represents a convolution with an odd function, for $C_2 = \cos kt$, we have

$$\begin{aligned} M(t_0) &= C_3 \sin kt_0 \int_{-\infty}^{\infty} \frac{e^{2r}\cos\varphi}{(e^r+1)^2(e^{2r}-1)} \sin ktdt \\ &= \sin kt_0 M(k). \end{aligned}$$

Since $\cos\varphi \propto \dot{r}(t)$, we can see that the above integral is the sine transform of an L^1 function.

$$\int_{-\infty}^{\infty}\left|\frac{e^{2r}\cos\varphi}{(e^r+1)^2(e^{2r}-1)}\right|dt = 2\int_0^{\infty}\left|\frac{e^{2r}\cos\varphi}{(e^r+1)^2(e^{2r}-1)}\right|dt$$
$$\leq \frac{C_3}{C_0}\int_{r(0)}^{r(\infty)}\frac{e^{2r}}{(e^r+1)^2(e^{2r}-1)}dr < \infty.$$

We know by the properties of the Fourier transform on $L^1(\mathbb{R})$ (see Katznelson p. 120-131), that $M_0(k)$ is a uniformly continuous function of k that is not identically zero. Thus there exists some interval $k_1 \leq k \leq k_2$ such that $M_0(k)$ is non-zero. For these values of k, $M(t_0)$ has simple zeros.

The Melnikov function in (x, y) coordinates:

We now consider the dynamical system

$$\dot{x} = (\gamma+\gamma')\cos^2\varphi - \frac{2\omega r\sin\varphi e^r}{(e^r+1)^2} + (\gamma+\gamma')\frac{e^{2r}+1}{e^{2r}-1}r\sin^2\varphi, \quad r \neq 0,$$
$$\dot{y} = (\gamma+\gamma')\cos\varphi\sin\varphi + \frac{2\omega r\cos\varphi e^r}{(e^r+1)^2} - (\gamma+\gamma')\frac{e^{2r}+1}{e^{2r}-1}r\sin\varphi\cos\varphi, \quad r \neq 0,$$

for $r \neq 0$

$$\dot{x} = \gamma+\gamma',$$
$$\dot{y} = 0,$$

for $r = 0$. Here $r = \sqrt{x^2+y^2}$, $\varphi = \tan^{-1}(y/x)$. We have the time periodic perturbation

$$\vec{g}(t,x,y) = \frac{\epsilon C_2(t) r e^r}{(e^r+1)^2}\begin{pmatrix}-\sin\varphi \\ \cos\varphi\end{pmatrix}.$$

The following analysis is for the case $\gamma+\gamma' = .1227$, the nondegenerate case can be studied in a similar fashion. We have

$$f \wedge g = (\gamma+\gamma')\cos\varphi C_2(t_0)\left(\frac{re^r}{(e^r+1)^2}\right)$$

$$trDf = (\gamma+\gamma'\cos\varphi\left(\frac{1}{r} - \frac{e^{2r}+1}{e^{2r}-1}\right), \quad r \neq 0,$$
$$= 0, \qquad r = 0,$$
$$e^{\int_0^t trDf ds} = \frac{2r(t)e^{r(t)}}{e^{2r(t)}-1}.$$

For $C_2(t) = \cos kt$, our Melnikov function is

$$\begin{aligned} M(t_0) &= -\int_{-\infty}^{\infty} \sin kt_0 \dot{r}(t) \sin kt \frac{r^2 e^{2r}}{(e^{2r}-1)(e^r+1)^2} dt \\ &= \sin kt_0 M_0(k). \end{aligned}$$

Again we see that $M_0(k)$ is a sine transform of an L^1 function:

$$\begin{aligned} &\int_{-\infty}^{\infty} \left| \frac{\dot{r}(t) r^2 e^{2r}}{(e^{2r}-1)(e^r+1)^2} \right| dt \\ &= \int_{r(0)}^{r(\infty)} \frac{r^2 e^{2r}}{(e^{2r}-1)(e^r+1)^2} dr \\ &= \int_{0}^{r(\infty)} \frac{r^2 e^{2r}}{(e^{2r}-1)(e^r+1)^2} dr \\ &< \infty. \end{aligned}$$

This is because $\frac{r^2 e^{2r}}{(e^{2r}-1)(e^r+1)^2}$ is bounded on the interval $(0, r(\infty)]$. We see that $M_0(k)$ is again the sine transform of an odd L^1 function so that there exists an interval $k_1 \leq k \leq k_2$ so that $M_0(k)$ is non-zero, giving us a Melnikov function with simple zeros.

Under such a periodic stretching, we find chaotic dynamics occurring in the phase portrait of the evolution equations for the ellipse. This indicates a sort of randomness in the evolution of the vortex. The phase portrait includes a horseshoe as a subsystem, which we know from chapter one indicates somewhat erratic behavior on an invariant set. Assuming the inability to make completely precise measurements, we can only predict what will happen to the vortex for a finite time, after this time we have no knowledge of how it will evolve.

Appendix

We present the details of the calculation of the following integral from chapter three via residues:

$$\int_{-\infty}^{\infty} \frac{e^{\gamma t} - e^{-\gamma t}}{(e^{\gamma t} + \beta + e^{-\gamma t})^2} \sin ktdt$$

which by a change of variables $\tau = \gamma t$ becomes

$$\frac{1}{\gamma} \int_{-\infty}^{\infty} \frac{e^{\tau} - e^{-\tau}}{(e^{\tau} + \beta + e^{-\tau})^2} \sin m\tau d\tau,$$

where $m = k/\gamma$. Consider the meromorphic function

$$\frac{(e^{3z} - e^{z})e^{imz}}{(e^{2z} - \beta e^{z} + 1)^2}.$$

The denominator has roots

$$e^{z} = \frac{\beta \pm \sqrt{\beta^2 - 4}}{2}$$

which can write as

$$= e^{\pm i\alpha},$$

since we know that $0 < \beta < 2$. Here, $\alpha = \cos^{-1}(\beta/2)$ which gives us $-\pi i/2 < \alpha\pi i/2$. Thus, our function

$$\frac{(e^{3z} - e^{z})e^{imz}}{(e^{z} - e^{i\alpha})^2(e^{z} - e^{-i\alpha})^2}$$

has double poles at $z = \pm i\alpha + 2\pi i N, \quad N \in \mathbb{Z}$. Let $r = z - (i\alpha + 2\pi i N)$. The integral is clearly odd in m. Consider the case $m > 0$. We have that

$$\begin{aligned}
&\text{Im}\frac{1}{\gamma} \int_{-\infty}^{\infty} \frac{e^{3\tau} - e^{\tau}}{(e^{2\tau} + \beta e^{\tau} + 1)^2} e^{im\tau} d\tau \\
&= \lim_{N\to\infty} \text{Im}\frac{1}{\gamma} \int_{-(2N+1)\pi}^{(2N+1)\pi} \frac{e^{3\tau} - e^{\tau}}{(e^{2\tau} + \beta e^{\tau} + 1)^2} e^{im\tau} d\tau \\
&= \lim_{N\to\infty} \text{Im}\frac{1}{\gamma} \left[\frac{1}{2\pi i} \sum_{0<y<(2N+1)\pi} \text{Res}\left(\frac{e^{3z} - e^{z}}{(e^{2z} + \beta e^{z} + 1)^2} e^{imz} \right) \right. \\
&\left. - \int_{|z|=(2N+1)\pi, y>0} \frac{e^{3\tau} - e^{\tau}}{(e^{2\tau} + \beta e^{\tau} + 1)^2} e^{im\tau} d\tau \right].
\end{aligned}$$

The last integral goes to zero as $N \to \infty$ so that for $m > 0$, we wish to calculate

$$\operatorname{Im}\left[\frac{1}{2\pi\gamma i}\sum_{y>0}\operatorname{Res}\left(\frac{e^{3z}-e^{z}}{(e^{2z}+\beta e^{z}+1)^2}e^{imz}\right)\right].$$

Using the fact that the integral is odd in m, we have that for all $m \neq 0$, the integral becomes:

$$\frac{m}{|m|}\operatorname{Im}\left[\frac{1}{2\pi\gamma i}\sum_{y>0}\operatorname{Res}\left(\frac{e^{3z}-e^{z}}{(e^{2z}+\beta e^{z}+1)^2}e^{i|m|z}\right)\right].$$

Thus we need to calculate the residues of the function in the upper half plane. We can calculate the coefficients of the Laurent expansion of the function by first considering the expansion of its components in the neighborhood of $i\alpha + 2\pi i N$. We have:

$$\begin{aligned}
e^{3z} &= e^{3i\alpha}(1+3r+\frac{9}{2}r^2+\dots)\\
e^{z} &= e^{i\alpha}(1+r+\frac{1}{2}r^2+\dots)\\
e^{imz} &= e^{-m\alpha-2\pi mN}(1+imr-\frac{m^2}{2}r^2+\dots)\\
(e^{z}-e^{i\alpha})^2 &= e^{2i\alpha}(r^2+r^3+\dots)\\
(e^{z}-e^{-i\alpha})^2 &= -4\sin^2\alpha+4i\sin\alpha e^{i\alpha}r+\dots
\end{aligned}$$

We write the function in the form:

$$\frac{1}{r^2}\left(\frac{a+br+\dots}{c+dr+\dots}\right)$$

which has the Laurent expansion

$$\frac{a}{c}r^{-2}+\left(\frac{b}{c}-\frac{da}{c^2}\right)r^{-1}+\dots$$

so that the residue at $r=0$ is $\frac{b}{c}-\frac{da}{c^2}$. Here

$$\begin{aligned}
a &= (e^{3i\alpha}-e^{i\alpha})e^{-m\alpha-2\pi mN},\\
b &= e^{-m\alpha-2\pi mN}[im(e^{3i\alpha}-e^{i\alpha})+3e^{3i\alpha}-e^{i\alpha}],\\
c &= e^{2i\alpha}(-4\sin^2\alpha),\\
d &= e^{2i\alpha}(4ie^{i\alpha}\sin\alpha-4\sin^2\alpha).
\end{aligned}$$

Let R_x denote the residue at the point x. Then,

$$R_{i\alpha+2\pi iN} = \frac{-e^{-m\alpha-2\pi mN}m}{2\sin\alpha}$$

Notice that $R_{i\alpha+2\pi iN} = R_{i\alpha}e^{-2\pi Nm}$. A similar calculation shows that

$$R_{-i\alpha+2\pi iN} = \frac{e^{m\alpha-2\pi mN}m}{2\sin\alpha}.$$

Thus, our integral becomes:

$$\frac{1}{2\pi\gamma}\left[\frac{e^{-|m|\alpha}m}{2\sin\alpha} - \frac{m\sinh m\alpha}{\sin\alpha}\frac{e^{-2\pi mN}}{1-e^{-2\pi mN}}\right]$$

Bibliography

Ahlfors, L.V. [1979] *Complex Analysis* New York: McGraw-Hill, Inc.

Arnold, V.I. [1984] *Mathematical Methods of Classical Mechanics* New York: Springer-Verlag.

Arnold, V.I. and Avez, A. [1968] *Ergodic Problems of Classical Mechanics* New York and Amsterdam: W.A. Benjamin, Inc.

Bayly, B. [1986] *Kinematics and Dynamical Problems in Three Dimensional Steady Flows* Ph. D. Thesis, Princeton University.

Birkhoff, G. D.[1935],"Nouvelles Recherches Sur les Systèmes Dynamiques," *Mem. Pont Acad. Sci. Novi Lyncaei,* **1**, 85-216.

Chorin, A.J. and Marsden, J.E. [1979] *A Mathematical Introduction to Fluid Mechanics* New York: Springer-Verlag.

Guckenheimer, J. [1979] "A Brief Introduction to Dynamical Systems" *Lectures in Applied Math.* **17**, 187-252.

Guckenheimer, J. and Holmes, P. [1983] *Nonlinear Oscillations, Dynamical Systems, and Bifurcations of Vector Fields*, Springer-Verlag, New York.

Hartman, P. [1982] *Ordinary Differential Equations*, Boston, Basel, Stuttgart: Birkhäuser.

Hirsch, M.W. and Smale, S. [1974] *Differential Equations, Dynamical Systems, and Linear Algebra*, New York: Academic Press.

Holmes, P.J. [1980] "Averaging and Chaotic Motions in Forced Oscillations", *SIAM J. Applied Math* **38**, No. 1, February, pp.68-80.

Holmes, P.J. [1981] "Space and Time Periodic Perturbations of the sine-Gordon Equation", *Dynamical Systems and Turbulence*, D.A. Rand and L.-S. Young (eds.) Springer Lecture Notes in Mathematics, Springer Verlag: New York, Berlin. Vol. 89.

Holm, Marsden, and Ratiu [1979] "Nonlinear Stability of the Kelvin-Stuart Cat's Eyes Flow", *AMS Proceedings of Math. Bio. Symposia and Summer Seminars.* July, 1979.

Katznelson, Y. [1976] *An introduction to Harmonic Analysis* New York: Dover Publications Inc.

Kida, S. [1981] *Journal of the Physical Society of Japan* **50**, No. 10, October, pp. 3517-3520.

Lamb, H. [1945] *Hydrodynamics.* New York: Dover Publications.

Majda, A. [1986] *Princeton University: Lectures on Incompressible Fluid Flow-Fall 1986.*

Marsden, J.E. "Chaotic Orbits by Melnikov's Method: a Survey of Applications", PAM-173/COMM , Center for Pure and Applied Math., University of California, Berkeley. August, 1983.

Melnikov, V.K. [1963]. "On the Stability of the Center for Time Periodic Perturbations." *Trans. Moscow Math Soc.,* **12**, 1-57.

Moser, J. [1973]. *Stable and Random Motions in Dynamical Systems.* Princeton University Press: Princeton.

Moore, D.W. and Saffman, P.G. [1975] "The Density of Organized Vortices in a Turbulent Mixing Layer" *Journal of Fluid Mechanics* **69**, part 3, pp. 465-473.

Neu, J.C. [1983]. "The Dynamics of a Columnar Vortex in an Imposed Strain" *MRSI* **022-83**.

Neu, J.C. [1984]. "The Dynamics of Stretched Vortices" *Journal of Fluid Mechanics* **143**, pp. 253-276.

Palis, J. [1969] " On Morse-Smale Dynamical Systems" *Topology* **8**, 385-405.

Pedlosky, J. [1982] *Geophysical Fluid Dynamics* New York: Springer-Verlag.

Prudnikov, A.P., Brychkov, Y.A., and Marichev, O.I. [1986] *Integrals and Series: Vol. I Elementary Functions.* Translated from Russian by N.M. Queen. New York: Gordon and Breach Science Publishers.

Smale, S. [1963]. "Diffeomorphisms with many Periodic Points." *Differential and Combinatorial Topology*, S.S. Cairns (ed.), pp. 63-80. Princeton University Press: Princeton.

Stuart, J.T. [1971]. "Stability Problems in Fluids." *AMS Lectures in Applied Math.* **13**. pp.139-155.

Van Dyke, M. [1982] *An Album of Fluid Motion.* Stanford, CA: The Parabolic Press.